FIFTH RARE EARTH RESEARCH CONFERENCE

AUGUST 30, 31, SEPTEMBER 1, 1965

Book Six

solid state session P-3

sponsored by Institute for Atomic Research, Iowa State University and Air Force Office of Scientific Research - Directorate of Chemical Sciences

DISCLAIMER NOTICE

THIS DOCUMENT IS BEST QUALITY PRACTICABLE. THE COPY FURNISHED TO DTIC CONTAINED A SIGNIFICANT NUMBER OF PAGES WHICH DO NOT REPRODUCE LEGIBLY.

CONTENTS

Solid State Session P-3

EXCHANGE INTERACTIONS IN RARE EARTH METALS.

R. J. Elliott

Clarendon Laboratory,
Oxford, England.

ABSTRACT

The complex magnetic orderings observed in the rare earth metals may be understood phenomenologically[1] in terms of an effective exchange interaction $J(\underline{R})$ between the localised 4f electrons a distance $\underline{R}$ apart which is of long range so that the Fourier transform

$$J(\underline{q}) = \sum_{R} J(\underline{R}) e^{i\underline{q}\cdot\underline{R}}$$

has a maximum for $\underline{q}$ at some general point in the Brillouin Zone. The anisotropy of the systems can be understood in terms of the crystalline electric field which influences the orbital motion of the f electrons. In the second half of the rare earth series the crystal field effects are comparable to the exchange energy, in the first half they are somewhat larger. The detailed form of $J(\underline{q})$ and of the anisotropy terms can be studied through the spin-wave spectra which are very complex in these complicated magnetic structures[2]. The details of the magnetic ordering are found by neutron diffraction to change with temperature T

and with alloying[3] partly because of the anisotropy, but also because the effective $J(\underline{q})$ appears to change with T.

The origin of the exchange interaction is believed to lie in indirect exchange through the conduction electrons.[4] A nearly free electron calculation gives the correct essential properties of $J(\underline{q})$[5] although the actual Fermi surface must be very different to this[6] and the effect is enhanced by the interelectronic interaction[7]. When magnetic ordering sets in the conduction electrons see an exchange field of a new symmetry which causes gaps to appear in the one-electron energy spectrum. These gaps follow new zone boundaries which tend to form near the Fermi surface. The subsequent distortion of the Fermi surface gives rise to strong anomalies in electrical transport properties like the resistivity, and in optical absorption. It also causes a change in $J(\underline{q})$ due to the redistribution of electrons.[8] Furthermore the scattering of the conduction electrons off the spin disorder causes a modification of the conduction electron polarisation which changes $J(\underline{q})$[9]. These mechanisms give a reasonable explanation of the observed variations.

Thus the combination of indirect exchange and crystal field effects appears to account qualitatively for the complex properties of the rare earth metals. A more detailed test of the theory awaits more experimental data

on $J(q)$ and on the precise form of the Fermi surface.

References.

1. For a review see R. J. Elliott Magnetism II, 385 (1965) [Ed. Rado and Suhl: Academic Press].
2. B. R. Cooper et al Phys. Rev. 127, 57 (1962); 131, 1043 (1963).
3. W. C. Koehler et al Proc. 3rd Rare Earth Conf. Clearwater Fla. 1963 [Gordon and Breach].
4. For a review see T. Kasuya Magnetism II (1965) [Ed. Rado and Suhl: Academic Press.]
5. K. Yosida and G. Watabe Prog. Theor. Phys. 28, 361, (1962).
6. A. J. Freeman and P. O. Dimmock Phys. Rev. Lett. 13, 750 (1964).
7. A. W. Overhauser Phys. Rev. 128, 1437 (1962); J. Appl. Phys. 34, 1019, (1963).
8. R. J. Elliott and F. G. Wedgwood. Proc. Phys. Soc., 84, 63 (1963).
9. P. G. de Gennes J. Phys. Rad. 23, 260 (1962).

   H. Miwa Proc. Phys. Soc. (1965 to appear).

SOME THEORETICAL ASPECTS OF HEAVY RARE EARTH METALS

Takeo Nagamiya

Faculty of Engineering Science
Osaka University
Toyonaka, Japan

The band structure for the conduction electrons and its consequence on the magnetic and electric properties of heavy rare earth metals are discussed. A brief description of the theory of the magnetization processes of a helical spin arrangement, in particular structure changes from helix to fan and then to ferromagnetic alignment with increasing magnetic field, is presented, the temperature being assumed to be finite and a sixfold anisotropy within the easy plane being included. Further, spin waves in a helical arrangement and in a fan arrangement are discussed; uniform modes and their frequencies are particularly considered.

1. Introduction

The theoretical understanding of the magnetic and electric properties of rare-earth metals is at present made through two lines of approach. (a) One assumes for the conduction electrons the picture of the free electrons perturbed by the periodic lattice potential, or of electrons in bands that would follow with the single orthogonalized plane wave (SOPW) functions. Then, one considers the exchange and Coulomb interactions between the conduction electrons and the 4f shells. On this basis, one can understand roughly, but consistently, the ferromagnetism of Gd, the helical ordering of the 4f moments in heavier metals, the period of this ordering, its dependence on atomic number and

temperature, the electrical resistivity as a function of temperature and ordering, and so on (Kasuya[1] 1964). However, reliable calculations of the band structure and experimental determinations of the Fermi surface are not yet available, which puts a difficulty in the way of a further theoretical study. (b) One assumes certain constants of the indirect exchange coupling among the 4f moments and also certain forms of the anisotropy energy for each 4f moment which depend on the 4f shell electronic configuration. One can then discuss the various moment orderings observed or predictable for rare-earth metals. One can also discuss the temperature and magnetic-field dependence of the ordering, as well as the spin wave spectra (Kaplan,[2] Elliott,[3] Miwa and Yosida[4] 1961; Nagamiya et al.[5] 1962, Kitano and Nagamiya[6] 1964; Cooper et al.[7,8] 1962, 63). However, the values of the theoretical parameters have to be sought ultimately in the interaction between the 4f shells and the conduction electrons, and for this purpose one has again to know the band structure. Also, experimental data are not sufficiently available to determine these parameters.

In this note, the theory of the type of (a), which is inevitably qualitative, will be briefly discussed, and then the writer's theory of the type of (b) of the magnetization processes in heavy rare-earth metals will be described, though not fully. Besides, the modes and frequencies of the spin waves in helical and fan spin-structures, particularly of those which are to be resonant to external, homogeneous, oscillating magnetic field, will be presented, in a more complete and correct form than those published earlier by Cooper et al.

2. Conduction Band and Magnetic and Electric Properties

In the early theory of Yosida and Watabe[9] the conduction electrons were assumed to be free at the starting point and then the f-s exchange interaction was introduced as a

perturbation. When the f-shell moments are aligned helically, there appear energy-gap planes in the k-space for the conduction electrons. If the wave vector, Q, of this helical order is such that a certain set of the gap planes come to tontact with the Fermi surface, then the helical order is stabilized. It was found that such planes are those which perpendicularly bisect the vectors $K_{111}+Q$ drawn from the origin. Here the index 111 refers to the orthorhombic unit cell for the h.c.p. lattice, and there are altogether six equivalent indices of this kind. Q was found to be in the c-direction and to correspond to a period of approximately seven hexagonal layers. Thus, their theory appeared to work nicely.

If we are allowed to treat both the lattice potential and the exchange potential as perturbations, then we shall find that the energies arising from these two are additive, as far as the second order perturbation energies are concerned; thus, the theory of Yosida and Watabe will be validated. In the theory of SOPW, there is a theorem that the kinetic energy increase of an electron in a SOPW state due to the core functions, added to a plane wave function for the purpose of orthogonalization, approximately cancel the potential energy decrease due to the core potential. If this cancellation is nearly perfect, then we have an energy spectrum of a nearly free electron, and we can validate the Yosida-Watabe theory.

However, observations of the electronic specific heats of some rare-earth metals, as well as of Y and Sc, show that they have values seven times as large as that one would expect with the assumption of free electrons. The conduction electrons must, therefore, be strongly perturbed by the lattice periodic potential. Fig.1 shows the $(1\bar{1}0)$ cross-section of the Fermi sphere for free electrons and of the Brillouin zone boundaries. An expected distortion of the Fermi surface due to the lattice periodic potential is also

shown. In the reduced zone scheme, this distorted Fermi surface will be as shown in Fig.2. One will see by a consideration in three dimensions that there are, in addition, electron-filled hemispheres on the top and bottom surfaces of the hexagonal cylinder (Fig.3) and holes at the midpoints of the vertical edges of this cylinder (not shown in the figure).

We assume that the cancellation, mentioned before, is less perfect, thus the distortion of the Fermi surface greater, for heavier metals; in particular, the portion of the Fermi surface at the central part of Fig.2 is assumed to be flatter for heavier metals. If one considers this portion only and studies the q-dependent susceptibility(q being the wave vector of a hypothetical magnetic field which varies in space with a wave vector q), then one will see that the

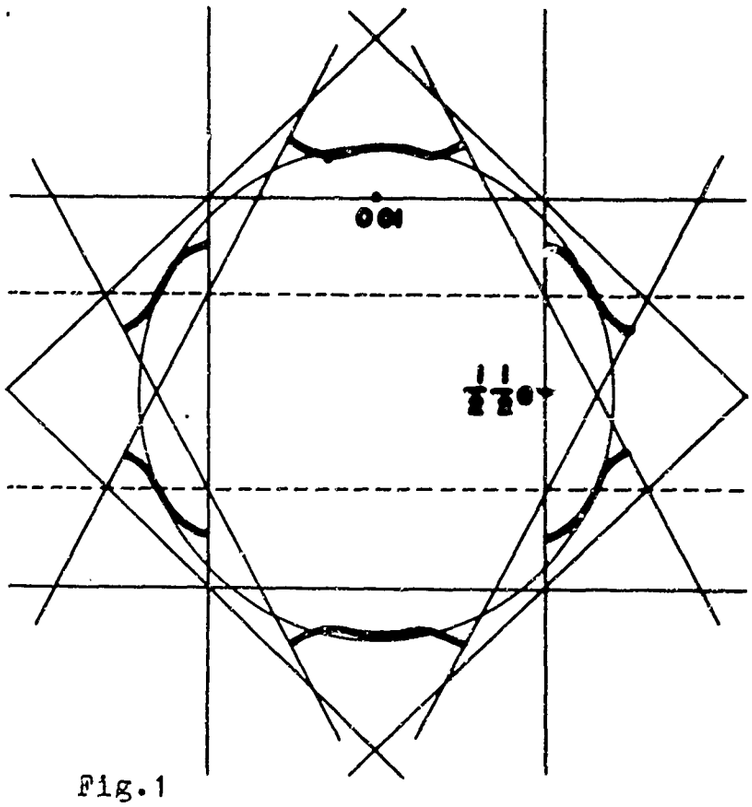

Fig.1

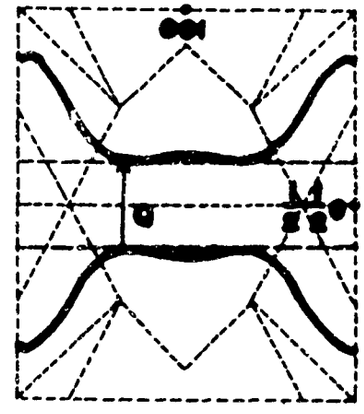

Fig.2

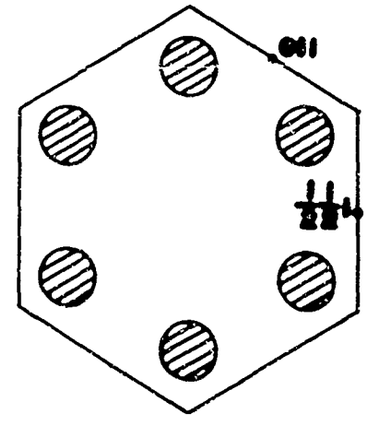

Fig.3

q-dependent susceptibility has a maximum at q=Q, where Q is a vertical vector shown in Fig.2. This would mean that a helical order having a wave vector Q stabilizes itself by producing gap planes which contact the Fermi surface as shown by horizontal broken lines also in Fig.2 (one plane is produced by one kind of spin, the other by the other kind of spin). The heavier the metal, the flatter will be this portion of the Fermi surface, hence greater will be the value of Q. This is in accordance with the observation of the wave number of the ordered arrangement in heavy rare-earth metals immediately below the Néel temperature. With decreasing temperature, the magnitude of the energy gap will increase, and the flat part of the Fermi surface contacted by the gap plane will be replaced, more or less completely, by this plane. Then, in order to minimize the total energy, the increase in the energy gap will cause Q diminish, the opposite Fermi surface being pushed away; this may be seen by a simple calculation for a one-dimensional system having a parabolic energy spectrum. Thus, Q decreases with decreasing temperature, as boserved.

When one has a sinusoidal order, as in Er and Tm, both the upper and lower gap planes appear for each kind of spin, and they will behave as boundaries for the electron-filled region. The value of Q, therefore, will not change with decreasing temperature. Of course, the actual situation may not be so simple. In particular, the appearance of harmonics in the periodic order will certainly play an important role in fixing the period to an integral number of layers[10] (seven layers in the cases of Er and Tm).

We have so far neglected other portions of the Fermi surface. Including the small electron surfaces shown in Fig.3 and the hole surfaces, they will contribute a decreasing function of $|q|$ to the q-dependent susceptibility when q varies in the c-direction. In Gd, in which the maximum at q=Q in the aforethought susceptibility may be assumed to be

the least, this contribution might smear it out or make it the second maximum. If this is the case, we expect ferromagnetism for Gd.

The anisotropy of the Fermi surface of the sort considered above is further supported by the fact that, in the paramagnetic temperature range, the resistivity parallel to the c-axis is smaller than that perpendicular to the c-axis (less average effective mass in the c-direction than perpendicular to it). This anisotropy in the resistivity increases with increasing atomic number, as expected. A hump in the resistivity parallel to c versus T curve, observed near T_C in Gd and near T_N in some heavier metals, may be interpreted as being due to short range spin order that corresponds to Q. Further anomalies at lower temperatures can naturally be interpreted as being due to long range order and the consequent decrease in the free Fermi surface.[11,12]

Kasuya[1] discusses quantitatively all these features and others, but the present writer feels that we cannot go much further at present than the qualitative discussion given in this section.

3. Structure Changes of a Helical Spin Arrangement by External Magnetic Field

It has been known since some years ago that a helical spin ordering, when subjected to a magnetic field applied in the easy plane in which the spin vectors rotate, changes discontinuously to a fan-like ordering when the field exceeds a certain critical value and further, above another critical field the latter transforms to a parallel alignment. The theory was put forward by Herpin and Mériel[13] and Nagamiya et al.[5] They confined themselves to T=0. The theory for finite T and for various modifications of the helical ordering was then worked out by Kitano and Nagamiya.[6]

We shall discuss here only the case of helix-fan-ferro transitions. The temperature may be finite and an aniso-

tropy energy of sixfold symmetry in the easy plane may be included. The applied field be in the easy direction in the plane. The mathematics presented here is different from that of reference 6.

Denoting by H_n^* (vector) the effective field acting on the nth spin, by $S\sigma_{ni}$ the thermal average of the spin component S_{ni} (i=x,y,z), and by w_n the anisotropy Hamiltonian of the nth spin which is a function of S_n, namely $w_n=w(S_n)$, we can write the molecular field equation as

$$S\sigma_{ni}= Tr[S_i exp(kT)^{-1}(H_n^*\cdot S-w_n)]/Tr[exp(kT)^{-1}(H_n^*\cdot S-w_n)]. \quad (1)$$

We want to solve this equation.

To study the stability of the ferromagnetic alignment along the applied field, whose direction will be taken as x, we put $\sigma_{nx}=\sigma_0+\sigma'_{nx}$ and assume that σ'_{nx}, σ_{ny}, and σ_{nz} to be small (the easy plane is taken as the xy-plane). Here σ_0 is assumed to satisfy the equations

$$S\sigma_0= Tr[S_x exp(kT)^{-1}(H_0^* S_x-w_n)]/Tr[exp(kT)^{-1}(H_0^* S_x-w_n)], \quad (2)$$

$$H_0^*= \Sigma_m\ 2J_{mn}S\sigma_0 + H = 2J(0)S\sigma_0 + H. \quad (3)$$

J_{mn} is the exchange constant between S_m and S_n. For the y and z components, we have

$$H_{ny}^*= \Sigma_m\ 2J_{mn}S\sigma_{ny}, \quad H_{nz}^*= \Sigma_m\ 2J_{mn}S\sigma_{nz}. \quad (4)$$

For the x-component we put

$$H_{nx}^*= H_0^* + H_{nx}'^*, \text{ then } H_{nx}'^*= \Sigma_m\ 2J_{mn}So'_{nx}. \quad (5)$$

We want to linearize Eq.(1) with respect to σ'_{nx}, σ_{ny}, σ_{nz} and thus to $H_{nx}'^*$, H_{ny}^*, H_{nz}^*.

Before doing that, we specialize the anisotropy Hamiltonian as follows:

$$w_n= DS_{nz}^2 - (G/36S^4)[(S_{nx}+iS_{ny})^6+(S_{nx}-iS_{ny})^6]. \quad (6)$$

In the classical limit, we may put $S_{nx}= S\cos\varphi_n$, $S_{ny}= S\sin\varphi_n$, when the spin is in the xy-plane; then, the second term of

(6) reduces to $GS^2\varphi_n^2$. Also, when expanded in powers of $S-S_{nx}$ and S_{ny}, this term can be written to the lowest order as

$$\text{const} + \tfrac{1}{3}GS(S-S_{nx}) + \tfrac{2}{6}GS_{ny}^2.$$

Now, linearizing Eq.(1), we may obtain equations of the form

$$S\sigma_{ny} = H^*_{ny}B, \quad S\sigma_{nz} = H^*_{nz}C, \quad S\sigma'_{nx} = H'^*_{nx}A. \tag{7}$$

where A, B, C are functions of H_0^*/kT divided by kT. They represent certain susceptibilities along the x, y, z directions, respectively. It can be shown, as might be expected, that for D greater than G (both positive) B is the largest, C medium, and A the smallest. This means that the ferromagnetic alignment in the x-direction is the least stable for spin deviations in the y-direction. Therefore, we put in the first equation of (7) $\sigma_{ny} = \sigma_y \exp(iq\cdot R_n)$, where R_n is the position of the nth spin. Then we find, using the first equation of (4),

$$\sigma_y = 2J(q)B\sigma_y, \quad \text{where} \quad J(q) = \Sigma_m J_{mn}\exp(iq\cdot R_{mn}). \tag{8}$$

Here $R_{mn} = R_m - R_n$.

From (8) one may see that the ferromagnetic alignment in the x-direction becomes unstable when the applied field becomes less than the field, H_c, at which $2J(q)B=1$. Below this field an oscillation in the y-component of the spins will set in with a wave vector q. The quantity B can be calculated to be $S\sigma_0/(H_0^* + 2S\sigma_0 G)$, which is a decreasing function of H. Thus, the actual critical field, below which the ferromagnetic alignment becomes unstable, namely, the largest possible field consistent with $2J(q)B=1$, must correspond to the maximum of J(q). The value of q which gives this maximum is exactly the wave vector, Q, of the helical ordering. (We assume that the function J(q) is not affected by changes in the spin ordering, which may not be true in the actual case.) Thus, putting q=Q, we obtain

$$H_c = 2S\sigma_0[J(Q)-J(0)-G]. \tag{9}$$

here we used Eq.(3) to rewrite $2J(Q)B=1$. ($g\mu_B$ was assumed to be unity in the present notation; to convert to the ordinary notation, H is replaced by $g\mu_B H$.)

We have seen that the spin vectors oscillate in the xy-plane with the wave vector Q in the field below H_c. This oscillation is a static one, namely an oscillation in space. The spin vectors form a fan. Its amplitude, hence also the susceptibility of the fan structure for variations of the static field, H, in the x-direction can be calculated. For T=0, the susceptibility is ($g^2\mu_B^2$ times)

$$1/[3J(Q)-2J(0)-J(2Q)-35G]. \qquad (10)$$

It may be noted that this quantity can become negative when G increases. If this happens, the above argument fails. One expects in this case a transition of the first kind (discontinuous transition) between the fan and ferromagnetic structures at a field greater than that given by (9). In fact, a discontinuous transition was found by Kitano and Nagamiya in a certain range of G with complicated calculations, including numerical computation. One has even a discontinuous transition between the helical and ferromagnetic structures without an intermediate fan structure when G is sufficiently large, while for smaller G double transitions helix-fan-ferro are predicted. Koehler observed two intermediate fan structures in Ho in a certain range of temperature, but this is not yet understood theoretically.

4. Spin Waves in the Helical and Fan Structures

Spin waves in the helical spin arrangement, studied first by Yoshimori,[14] have the following characteristic. The mode for q=0 is a mere rotation of the system about the axis of the helix, provided that there is no anisotropy in the plane of spin rotation. Its frequency is therefore 0. For long waves, the spin wave frequency is proportional to the wave number. It then drops to a minimum near q=Q when

the out-of-plane anisotropy constant is small. When the latter is zero, then the minimum is also zero. This can be seen by considering the mode for q=Q. This mode is such that the spin at R_m and the spin at R_n oscillate with a phase difference of $Q \cdot R_{mn}$, so that the spins pointing opposite to each other oscillate with a phase difference of π; the plane spanned by the spin vectors performs a tilting motion. Assuming an anisotropy energy DS_{nz}^2, its frequency can be calculated to be

$$\hbar\omega_Q = 2S\{D[J(Q)-J(0)-J(2Q)]\}^{1/2}.$$

There are actually two degenerate modes corresponding to q=Q and q=-Q, which rotate opposite to each other. If a field is applied in the plane, in the x-direction, the frequency will split into two, one corresponding to the cos-mode in which the spins in the x-direction have the largest amplitude and the other to the sin-mode in which the spins perpendicular to the x-direction have the largest amplitude. The frequency of the q=0 mode has been shown to increase as H^2. When the field is above H_c, so that we have a ferromagnetic alignment, the mode for q=0 is just the ordinary resonance mode having a finite frequency. A peculiar fact is that the frequency of the ferromagnetic spin wave with a wave number Q vanishes at H_c, which could be imagined from that a fan structure with Q starts to develop at this field.

In the fan region for $H < H_c$, bith the modes for q=0 and q=Q have interesting features. Q and -Q are mixed to give a cos-mode and a sin-mode, of which the former has a vanishing frequency. In the cos-mode, the spin vectors at the center of the fan oscillate in the plane with the largest amplitude and the spins at the edges of the fan are at rest (Fig.4a). When one sees the vectors opposite to the field direction, one sees a sinusoidal curve for the locus of the top of the vectors; with the oscillation of the vectors this sinusoidal curve will shift up and down as illustrated in

Fig.4b. Thus, evidently, the frequency must vanish.

In the sin-mode, the frequency varies as $(H_c - H)^{1/2}$, namely, it is proportional to the angular amplitude of the fan. Denoting the latter by α, we can write the frequency as

$$\hbar\omega_{Q,\sin} = S\alpha\{[3J(Q)-2J(0)-J(2Q)-35G+N_x][D-(5/6)G]\}^{1/2},$$

provided that α is small and the transition between the fan and the ferromagnetic alignment is of the second order. Here N_x is the demagnetizing coefficient in the x-direction, multiplied by $(g\mu_B)^2 N$, N being the number of atoms in unit volume. This mode is illustrated in Fig.5a and 5b.

The mode for q=0 is such that the spin vectors describe equal ellipses in space, so that the fan oscillates as a rigid body in the easy plane and, with a phase difference of $\pi/2$, oscillates in the direction perpendicular to the easy plane with some bending, like an ordinary fan oscillates when people use it to produce breeze. Its frequency is given by

$$\hbar\omega_0 = 2S[(A_0+B_0)(A_0-B_0)]^{1/2},$$

where

$$A_0+B_0 = J(Q)-J(0)-\tfrac{1}{4}\alpha^2[J(Q)-J(0)+35G]-(2S)^{-1}(H_c-H) + \tfrac{1}{2}N_y(1-\tfrac{1}{2}\alpha^2),$$

$$A_0-B_0 = J(Q)-J(0)+(D+\tfrac{1}{6}G)-G+\tfrac{1}{4}\alpha^2[J(Q)-J(0)-5G] - (2S)^{-1}(H_c-H)+\tfrac{1}{2}N_z.$$

References

1. T. Kasuya, Technical Report of ISSP, Ser.A, No.123 (1964)
2. T. A. Kaplan, Phys. Rev. 124, 329 (1961)
3. R. J. Elliott, Phys. Rev. 124, 346 (1961)
4. H. Miwa and K. Yosida, Progr. Theoret. Phys. (Kyoto) 26, 693 (1961)
5. T. Nagamiya, K. Nagata, and Y. Kitano, Progr. Theoret. Phys. (Kyoto), 27, 1253 (1962)

6. Y. Kitano and T. Nagamiya, Progr. Theoret. Phys. (Kyoto) 31, 1 (1964)
7. B. R. Cooper, R. J. Elliott, S. J. Nettel, and H. Suhl, Phys. Rev. 127, 57 (1962)
8. B. R. Cooper and R. J. Elliott, Phys. Rev. 131, 1043 (1963)
9. K. Yosida and A. Watabe, Progr. Theoret. Phys. (Kyoto) 28, 361 (1962)
10. T. Nishikubo and T. Nagamiya, J. Phys. Soc. Japan 20, May issue (1965)
11. H. Miwa, Progr. Theoret. Phys. (Kyoto) 28, 208 (1962); Tech. Rep. ISSP, Ser.A, No.69 (1963)
12. A. R. Mackintosh, Phys. Rev. Letters 9, 90 (1962)
13. A. Herpin and P. Mériel, C. R. Acad. Sci. 250, 1450 (1960); J. phys. rad. 22, 337 (1961)
14. A. Yoshimori, J. Phys. Soc. Japan 14, 807 (1959)

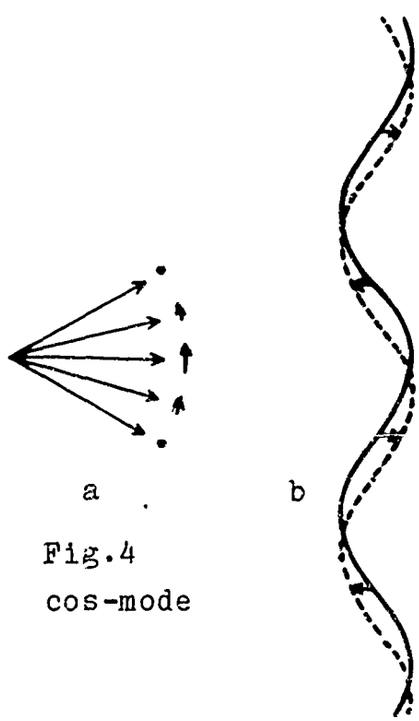

Fig.4
cos-mode

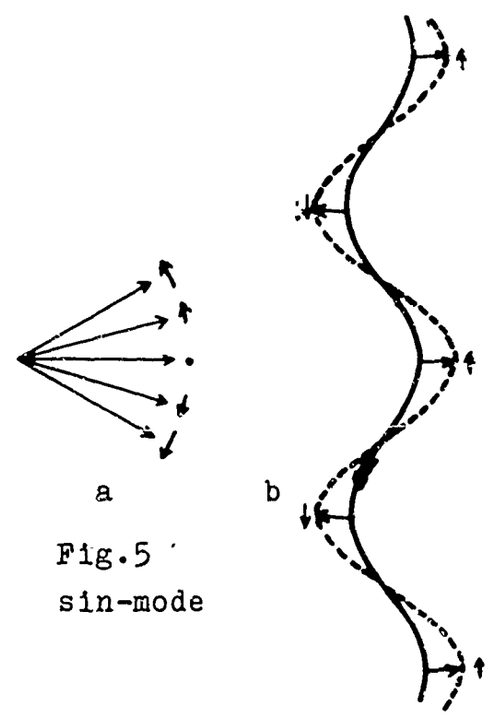

Fig.5
sin-mode

Experimental Study of the Excitations in Rare-Earth Metals

A. R. MACKINTOSH

Institute for Atomic Research and Department of Physics
Iowa State University, Ames, Iowa

Those properties of the rare earth metals which are of particular interest to the solid state physicist are primarily determined by the presence of a well-defined magnetic moment on the ion. The ordering of these localized moments below characteristic temperatures can have a profound effect on the conduction electrons, while the spin wave excitations from the magnetic ground state are of great importance in determining the thermal, transport and magnetic properties of the metal. Considerable progress has been made recently, both theoretically and experimentally, in understanding these excitations and this paper is an attempt to review recent experimental developments.

A direct experimental study of the Fermi surface in the rare earth metals is rendered difficult by the technical problems of preparing pure single crystals and the more fundamental difficulty that the application of a magnetic field, upon which the most successful techniques depend, may modify the magnetic structure and hence the Fermi surface itself. The study of the angular correlation of the photons emitted when positrons annihilate with the electrons is a relatively crude technique, but it does not suffer from these limitations and recent measurements on single crystals of holmium[1] have shown clearly that the Fermi surface is highly anisotropic,

in agreement with the anomalously high electronic specific heat[2] and recently band structure calculations[3]. It is likely that such experiments, together with calculations, will soon lead to a reasonably accurate picture of the Fermi surface. In particular, it should readily be possible to test the widely accepted hypothesis that the Fermi surfaces of all the hexagonal close packed rare earths are closely similar. The modification of the electronic distribution by the magnetic ordering may be observed by this technique and also by infrared absorption measurements[4].

Less direct information on the conduction electrons and their interaction with the spin waves is given by the study of transport properties. The temperature[5] and magnetic field[6] dependence of the electrical resistivity support the view that the Fermi surface is anisotropic, and measurements along the c axis give an indication of the considerable modification of the electronic distribution by the superzone planes.[7] These planes apparently affect the resistivity in the basal plane very little, so that changes which occur at magnetic transitions reflect primarily the difference in electron-magnon scattering and give some information about the spin waves. The electron-magnon interaction apparently makes a large contribution to the low temperature thermoelectric power[8], through the mechanism of magnon drag. Some characteristics of the spin wave spectra can also be determined from the temperature dependence of the magnetization[9] and heat capacity[10].

The most direct and powerful method of measuring the magnon dispersion curves is by inelastic neutron scattering, but again experimental difficulties appear in the form of the high thermal neutron capture cross section of most of the rare earths. Experiments are currently being performed on inelastic neutron scattering in terbium[11], however, and it seems that it should also be possible to make a detailed study of holmium. Magnetic resonance also gives directly the spin wave energies at some wavevectors[12] and this technique should provide a valuable adjunct to neutron scattering, particularly when the latter is technically difficult.

It appears that a good description of the Fermi surface and spin wave spectra of some of the rare earths will soon be available, and it will then be possible to make quantitative calculations of those physical properties which depend upon the electrons, the magnons and their interaction.

REFERENCES

1. R. W. Williams and A. R. Mackintosh (to be published).
2. O. V. Lounasmaa, Phys. Rev. A134, 1620 (1964).
3. J. O. Dimmock and A. J. Freeman, Phys. Rev. Letters 13, 750 (1964).
   T. L. Loucks (to be published).
4. C. Chr. Schüler, Phys. Letters 12, 84 (1964).
5. D. L. Strandburg, S. Legvold, and F. H. Spedding, Phys. Rev. 127, 2046 (1962).
6. A. R. Mackintosh and L. E. Spanel, Solid State Communications 2, 383 (1964).
7. A. R. Mackintosh, Phys. Rev. Letters 9, 90 (1962).
   H. Miwa, Prog. Theor. Phys. 29, 477 (1963).
   R. J. Elliott and F. A. Wedgwood, Proc. Phys. Soc 84, 63 (1964).
8. L. R. Sill and S. Legvold, Phys. Rev. A137, 1139 (1965).
9. K. Niira, Phys. Rev. 117, 129 (1960).
10. B. R. Cooper, Proc. Phys. Soc. 80, 1225 (1962).
11. H. Bjerrum Møller (to be published).
12. B. R. Cooper and R. J. Elliott, Phys. Rev. 131, 1043 (1963).

THE INDIRECT EXCHANGE INTERACTION IN THE RARE EARTH METALS*

Frederick Specht

William Marsh Rice University

Houston, Texas

An exact calculation is given for the indirect exchange interaction in the rare earth metals. With a free electron gas model for the conduction band the isotropic and first order non-isotropic terms are obtained, and it is shown that the non-isotropic term gives sizeable contributions to the interaction between two ions. An estimate is made of the contribution of the anisotropy to the crystalline exchange energy for the ferromagnetic phase. The two ferromagnetic ordering patterns with moments along the c-axis and in the hexagonal plane are considered, and an energy difference in agreement with experiment is found to be of the order of ten per cent.

In the rare earth metals the principal interaction between the 4f shell electrons on different ions is the indirect exchange interaction via the conduction band. The methods used thus far in calculating this interaction have involved some type of approximation on the functional

dependence of $J(\vec{k},\vec{k}')$, the exchange integral between the 4f shell electrons and a conduction electron. The approximation used most frequently is to replace $J(\vec{k},\vec{k}')$ by a constant. With a spherically symmetric conduction band the leading term of the interaction (isotropic) then has the radial dependence given by the well known Rudderman-Kittel[1]-Kasuya[2]-Yosida[3] (RKKY) function $[(x\cos(x) - \sin(x))/x^4]$ where $x = 2k_F R$. (k_F is the Fermi wave vector of the conduction band and R is the distance between the ions.) A somewhat better approximation is to set $J(\vec{k},\vec{k}') = J(\vec{k} - \vec{k}')$. Using this approximation, Kaplan and Lyons[4] calculated the isotropic and first order non-isotropic terms of the interaction and showed that the radial dependence of both terms differs from the (RKKY) function. We have evaluated the interaction exactly and obtain results quite different from all previous calculations. Here we give an outline of the calculation and briefly consider the effect of the resulting interaction on the magnetic ordering.

According to the usual expression from second order perturbation theory the effective exchange Hamiltonian between ions a and b takes the form[4]

$$H_{ab} = \sum_{ij} \vec{s}_{ai} \cdot \vec{s}_{bj} \times J_{kk'} J(\vec{k},\vec{k}',\vec{l}_{ai}) J(\vec{k}',\vec{k},\vec{l}_{bj}) \qquad (1)$$

where $J_{kk'}$ denotes the integral operator

$$\int_0^{k_F} d^3k \int_{k_F}^{\infty} d^3k' \exp[i(\vec{k}-\vec{k}')\cdot\vec{R}_{ab}](k^2-k'^2)^{-1}$$

and where $J(\vec{k},\vec{k}', \vec{\ell}\,)$ is defined by the relation

$$\langle \ell m' | J(k,k',\ell) | \ell m \rangle = \iint d\vec{x}_1\, d\vec{x}_2 \times R(r_1)R(r_2)\frac{Y^*_{\ell m'}(\hat{x}_1)\, e^{-i\vec{k}\cdot\vec{r}_2}\, Y_{\ell m}(\hat{x}_2)\, e^{i\vec{k}\cdot\vec{r}_1}}{|\vec{x}_1-\vec{x}_2|}$$

R(r) is the 4f shell radial function, and $(\vec{s}_{ai}, \vec{\ell}_{ai})$ denote the (spin,orbital) angular momentum operators of the i'th electron on ion a. Σ_i' denotes a sum over all the 4f shell electrons of the appropriate ion. It is convenient to define the z axis in the direction of $\vec{R}_{ab}$.

The isotropic and first order non-isotropic terms are obtained by using the spherical expansions of $|x-x'|^{-1}$ and $\exp(i\vec{k}\cdot\vec{r})$ and retaining only the terms of the expansion of $\exp(i\vec{k}\cdot\vec{r})$ with zero magnetic quantum number to second order. $J(k,k', \vec{\ell}\,)$ then becomes a linear combination of the irreducible tensor operators $\mathcal{Y}_{oo}(\vec{\ell}\,)$ and $\mathcal{Y}_{2o}(\vec{\ell}\,)$. Substituting this expression for $J(k,k',\vec{\ell}\,)$ into Eq.(1) and neglecting the term containing $\mathcal{Y}_{2o}(\vec{\ell}_{ai})\,\mathcal{Y}_{2o}(\vec{\ell}_{bj})$, one obtains the exchange Hamiltonian

$$H_{ab} = \sum_{ij} \vec{s}_{ai}\cdot\vec{s}_{bj}\, Q$$

where Q is of the form

$$Q = J_{kk'} \sum_{\lambda\mu\nu} \left[I_{\lambda\nu}(k,k')\, I_{\mu\nu}(k',k) \right.$$

$$\left. \times f_{\lambda\mu\nu}(\cos k_\theta, \cos k'_\theta) \left[Y_{\nu 0}(\hat{l}_{a_i}) + Y_{\nu 0}(\hat{l}_{b_j}) \right] \right]$$

$(\nu = 0, 2)$

and where $I_{\lambda\nu}$ are integrals of the form

$$\int\int r_1^2\, dr_1\, r_2^2\, dr_2 \left[R(r_1)\, R(r_2)\, j_\ell(kr_1) \right.$$

$$\left. \times j_m(k'r_2)\, (r_<^n / r_>^{n+1}) \right]$$

The evaluation of the integrals $J_{kk'} I_{\lambda\nu} I_{\mu\nu} f_{\lambda\mu\nu}$ is straight forward. The integrations over k_φ, k'_φ, k_θ and k'_θ are trivial. The integrations over k and k' can be performed by expanding the four Bessel functions in a Taylor series. Each term of the expansion leads to integrals of the form

$$\int_0^\infty x^m \sin x\, (x^2 - a^2)^{-1}\, dx \quad \text{and} \quad \int_0^\infty x^n \cos x\, (x^2 - a^2)^{-1}\, dx$$

with m odd and n even. With a convergence factor these integrals become $\left[(\pi/2)\, a^{m-1} \cos(a) \right]$ and $\left[(-\pi/2)\, a^{n-1} \sin(a) \right]$ respectively. After regrouping the terms of the expansion, one obtains

$$J_{kk'} I_{\lambda\nu} I_{\mu\nu} f_{\lambda\mu\nu} = \eta \left\{ \frac{\cos x}{x^3} - \right.$$

$$\left. \frac{\sin x}{x^4} \left[A_{\lambda\mu\nu} + k_F\, \partial/\partial k_F \right] + \cdots \right\} I_{\lambda\nu}(k_F)\, I_{\mu\nu}(k_F)$$

$$x = 2 k_F R_{ab}$$

Using this procedure, we have evaluated the isotropic and first order non-isotropic terms. We evaluated the functions $I_{\lambda\nu}(k_F)$ and their derivatives by numerical integration with the Hartree-Fock 4f shell functions given by Freeman and Watson[5]. The resulting Hamiltonian is given by

$$H_{ab} = (\vec{S}_a \cdot \vec{S}_b)\Big\{ \frac{\cos x}{x^3} + 12.3 \frac{\sin x}{x^4} + \cdots + \alpha(0.3)\Big[\frac{\cos x}{x^3} - 6.4 \frac{\sin x}{x^4} + \cdots \Big] \times \Big[\mathcal{Y}_{20}(\vec{L}_a) + \mathcal{Y}_{20}(\vec{L}_b) \Big] \Big\} \qquad (2)$$

where $\mathcal{Y}_{20}(\vec{L}) = (\vec{L}\cdot\vec{n})^2 - L(L+1)/3$. $\vec{n}$ is the unit vector between the ions, and α is defined by the operator equivalence

$$\sum_i \mathcal{Y}_{1q}(\vec{s}_i)\mathcal{Y}_{2q'}(\vec{l}_i) \rightarrow \alpha \mathcal{Y}_{1q}(\vec{S})\mathcal{Y}_{2q}(\vec{L})$$

within the manifold of the 4f shell angular functions. $\vec{S}$ and $\vec{L}$ are the total spin and orbital angular momentum operators of the 4f shell. S, L and α are given in Table I for the last half rare earths.

From the values of α and L it is clear that the non-isotropic term gives a sizeable contribution compared with the isotropic term. Furthermore both the isotropic and the non-isotropic functions differ considerably from the (RKKY) function and for small values of R_{ab} the (RKKY)

Table I.

Rare Earth	S	L	α
Tb	3	3	-1/6
Dy	5/2	5	-1/15
Ho	2	6	-1/44
Er	3/2	6	1/33
Tm	1	5	1/6

function represents a very poor approximation to isotropic interaction.

In order to obtain an estimate of the effect of the anisotropy on the crystalline exchange energy we investigated the energy as a function of moment orientation for the ferromagnetic phase. Using an IBM 7040 we summed b in Eq. (2) over all ions of a hcp lattice inside the sphere centered at a and of radius equal to 50 nearest neighbor spacings. From the form of the anisotropy in Eq. (2) and from the symmetry of a hcp lattice the ferromagnetic energy depends only on the angle between the moments and the c-axis. The results of this calculation is given in Table II for the two extreme cases in which the moments are along the c-axis or in the hexagonal plane.

In Table II it can be seen that there is about a 10% difference in energy for the two orientations, and

Table II.

Rare Earth	Exchange Energy Along c-axis	Exchange Energy in Hex. Plane
Tb	-0.156	-0.175
Dy	-0.106	-0.121
Ho	-0.0704	-0.0750
Er	-0.0429	-0.0395
Tm	-0.0213	-0.0155

in each case the anisotropy favors the orientation which is observed experimentally with regard to whether the moments are aligned along the c-axis or in the hexagonal plane. Although there are other effects contributing to this such as crystal field terms, on the basis of the exchange energy alone one can explain the preferred direction of moment orientation.

Using a free electron gas model we have calculated exactly the isotropic and first order non-isotropic terms of the interaction, and on the basis of a simple ferromagnetic order pattern we have shown that the anisotropy contributes significantly. This calculation by no means represents the true physical picture since plane waves were used for the conduction electrons. Until an accurate treatment is done with the appropriate band functions the nature of the interaction will remain in doubt.

Acknowledgements

The author would like to express his gratitude to Professor G. T. Trammell for his guidance and encouragement during this work.

References

* Supported by the National Aeronautics and Space Administration.

(1) M. A. Rudderman and C. Kittel, Phys. Rev. 96, 99 (1954).

(2) T. Kasuya, Prog. Theor. Phys. 16, 45 (1956).

(3) K. Yosida, Phys. Rev. 106, 893 (1957).

(4) T. A. Kaplan and D. H. Lyons, Phys. Rev. 129, 2072 (1963).

(5) A. J. Freeman and R. E. Watson. Materials Research Laboratory Report No. 118, Ordinance Materials Research Office, Watertown Arsenal, Watertown, Massachusetts (1962). (unpublished)

EFFECTS OF DILUTE RARE-EARTH ADDITIONS ON THE ELECTRICAL CONDUCTIVITY OF CERIUM AT LOW TEMPERATURES*

F. W. Clinard, R. O. Elliott, and W. N. Miner

University of California, Los Alamos Scientific Laboratory,
Los Alamos, New Mexico

ABSTRACT

Two atomic percent of the various trivalent rare earths were dissolved in cerium, and the electrical resistivities of these dilute binary alloys evaluated in the range 1.5 to 297°K, in order to determine whether the various solute magnetic properties might be reflected in resistivity measurements. It was found that the γ and β phases at room temperature showed a roughly linear dependence of resistivities on atomic number of solute species, with a slight effect attributed to solute-solvent atomic size mismatches. At 4°K the resistivities of predominantly α phases were found to be influenced by the presence of small amounts of β, and predominantly β phases by small amounts of α. Spin-disorder resistivities for β phase were found to be a nearly linear function of atomic number of solute, and did not clearly reflect the influence of any solute magnetic parameters. A slight decrease in spin-disorder resistivities was noted in the direction of the heavier rare earth solutes.

INTRODUCTION

The element cerium can exist in three phases between room temperature and 0°K. After being annealed at high temperature, the room temperature crystal structure is fcc (γ phase), with a lattice constant of 5.16 Å. Cerium in this form has about 0.9 4f electron per atom. On

*Work performed under the auspices of the U. S. Atomic Energy Commission.

cooling, the γ phase transforms partially to the hcp β form, but the number of 4f electrons is unchanged. With further cooling, the untransformed γ phase undergoes an electronic transformation to a more dense fcc form, designated α phase. This structure has a lattice parameter of 4.85 Å, and about 0.4 4f electron per atom. With still further cooling, the β phase transforms to the α phase, thus undergoing both a crystallographic and an electronic transformation. These low-temperature cerium phases have been more completely described by Gschneidner.(1)

Repeated thermal cycling of annealed samples between room and liquid helium temperatures can increase the amount of β to the point where it is predominant in this temperature range.(2) The β phase of cerium transforms from the paramagnetic to the antiferromagnetic form, at 12.5°K.(3)

Previous experimental findings on cerium containing small amounts of other rare earths suggest that the electrical conductivity of such binary solid solution alloys may be a function of solute species. Gschneidner et al.(4) reported that the temperature of the $\gamma \rightarrow \alpha$ cerium transformation, which involves a change in electronic configuration is strongly dependent on the specific rare earth alloying element at the 2 a/o level. In explaining this effect, they postulated that the spin of the unpaired 4f solute atoms was primarily responsible for the observed dependence. Their conclusion resulted from the observation that the change in transformation temperature as a function of the atomic number of the rare earth solute was reciprocally related to the spin of the solute atoms. The mechanism by which transition temperatures were lowered was believed to involve an indirect interaction between the unpaired 4f electron of the cerium and those of the solute atoms via the conduction electrons.(4) This suggestion that conduction electrons might play a part in the observed variation of transformation temperature as a function of solute species in cerium led to the present experiment, in which the resistivity of cerium plus 2 a/o rare earth additions has been determined as a function of temperature between 1.5 and 297°K. The present paper deals with the resistivities of these dilute alloys at room

temperature and at liquid helium temperatures.* Data are reported as a function of atomic number of solute, in order to determine the possible effect of various solute magnetic parameters on the resistivities of the alloys. Phases considered are: γ at 297°K, β at 297°K, β at 4°K, and α at 4°K. Only the β alloys at 297°K were thought to be single phase (i.e., phase pure). The other phases listed were the predominant ones in two-phase mixtures.

It is worth emphasizing that the cerium alloys dealt with here were quite dilute. Only one solute atom was present for every 50 solvent atoms.

Only one other investigation of the effect of a series of dilute solutions of rare earths in another rare earth on the electrical resistivities of the alloys has come to our attention. Mackintosh and Smidt[5] have reported residual resistivities of lutetium containing small percentages of gadolinium, terbium, dysprosium, holmium and erbium. They concluded that the change in residual resistivity per atomic percent of solute added is a function of the factor $(g-1)^2J(J+1)$, where g is the Landé factor and J is the localized ionic moment of the solute.

EXPERIMENTAL PROCEDURE

The eleven alloys discussed here were made from cerium stock which was estimated by difference to be 99.75 w/o pure. The major metallic impurities were 0.1 w/o lanthanum, 0.05 w/o manganese, and 0.05 w/o iron. Major non-metallic impurities were 235 ppm carbon, 115 ppm hydrogen, 30 ppm nitrogen, and 80 ppm oxygen. The resistivity of the cerium stock at 3.96°K (the normal boiling point of liquid helium at Los Alamos) was 7.14 $\mu\Omega$-cm.

Most of the alloys were arc-cast, swaged from about 0.312 to 0.265 in. diameter, heat treated, and then machined into the final rod-shaped

*The effects of the normally trivalent rare earth solutes are reported here. The normally divalent elements europium and ytterbium will be discussed at a later date.

form. Final sample dimensions were 0.250 in. diameter by 1.125 in. long. Potential probe separations for electrical resistivity measurements were about 1.5 cm.

Arc-cast alloys containing dysprosium, erbium and thulium were not swaged, but were induction cast to the approximate final shape in a helium atmosphere. The casting technique was to force the molten alloy up into a 0.275 in. ID tantalum tube immersed in the melt, by means of helium admitted to the previously evacuated furnace (manometric casting method). The tantalum tube was subsequently machined from the casting, and the specimen reduced to its final dimensions by further machining after heat treatment.

The alloys were homogenized and annealed in the following manner. Each specimen was wrapped in tantalum foil and sealed within a Pyrex capsule under 0.3 atm of argon. The capsules were then placed in a furnace at 525°C (about 0.7 of the melting point) for approximately 300 hr. At the end of this period, the capsules were removed from the furnace and cooled rapidly (about 100°K/min) to room temperature. The specimens were then broken out of the capsules and machined to their final dimensions. Specimen densities were determined at this time, and these γ-phase values are reported in Table I.

The machined specimens, four at a time, were loaded into the copper block specimen holder of the resistivity apparatus, and their resistivities measured at 297°K. These data are reported as the gamma curve of Fig. 1(a).

Cooling to liquid helium temperatures was then carried out in the following manner. The assembly containing the specimens was pre-cooled rapidly in liquid nitrogen and, after the nitrogen had been removed, was quenched with liquid helium. The liquid nitrogen pre-cool was utilized to minimize subsequent liquid helium boil-off. The time required for cooling from 297 to 4°K was typically 2 hr. This rapid cooling was utilized to favor the formation of α. It has been reported that slow cooling enhances the formation of β phase,[6] which is slower than γ to transform to α on further cooling.[1]

Resistivity data taken at 4°K on such predominantly alpha-phase samples are shown by the "alpha" curve of Fig. 1(b). Pumping was then employed to reduce the temperature of the liquid helium to approximately 1.5°K. A resistance heater imbedded in the copper specimen holder was used to warm the specimens from this temperature to 297°K at about 0.5°K/min.

Specimens to be evaluated in the β-phase condition were given the following thermal cycling treatment after being heat treated and before being inserted in the resistivity apparatus. Each was sealed within a Pyrex capsule under 1 atm of helium and then thermally cycled 24 times from room - to liquid helium - to room temperature. The procedure for one cycle involved immersing the capsule in liquid helium, holding it in the liquid for 15 min, and then removing it for warming to room temperature over a 15 min period. Specimen densities were determined after 24 cycles, and these β-phase values are given in Table I.

The β samples prepared in the above manner were loaded into the apparatus and their resistivities measured at 297°K. These values are reported in the beta curve of Fig. 1(a). They were then slowly cooled at a rate of about 0.5°K/min to about 40°K, quenched with liquid helium, and the helium pumped to approximately 1.5°K. Specimen resistivities were determined at the liquid helium isotherm of 4°K and are given by the "beta" curve of Fig. 1(b). As was the case for the alpha specimens, the apparatus heater was utilized to warm the specimens to 297°K at a rate of about 0.5°K/min.

Resistivity data were taken manually during all runs, a potentiometric circuit[7] being utilized. Voltage drops, which were later converted to resistivities, were read with a Rubicon Type B potentiometer. The sensitivity of this circuit was such that resistivity changes as small as 5×10^{-8} ohms were reliably detected.

Two methods of measuring temperature were used. In the range between room temperature and 16°K, temperatures were obtained by averaging the results from two calibrated copper-constantan thermocouples whose measuring junctions were soldered to the copper specimen holder.

The accuracy was estimated to be ± 0.5°K. In the range between 50 and 1.5°K, a calibrated germanium resistance thermometer was used, which had an estimated accuracy of ± 0.1°K. Its temperature measuring element was clamped to the specimen holder.

RESULTS AND DISCUSSION

Measured resistivities of cerium-rich alloys at 297°K as a function of rare earth solute species are shown in Fig. 1(a). The lower curve represents samples in the annealed condition. Density measurements, shown in Table I, indicated that most of these specimens were primarily γ phase, although the observed trend toward increasing density with increasing atomic number of the solute was not continued for the solutes erbium, thulium and lutetium. This failure to follow the trend was attributed to the likely formation of a small amount of beta phase in these three alloys. The upper curve of Fig. 1(a) represents resistivities of the cerium alloy samples at 297°K after they had been thermally cycled 24 times to 4°K to transform them as completely as possible to β. The trend in density measurements (Table I) and subsequent resistivity-temperature curves indicated that the cycled specimens consisted entirely of β at room temperature. It may be seen in Fig. 1(a) that the resistivities of both γ and β phases are linear functions of the atomic numbers of rare earth solutes.

The results shown in Fig. 1(a) indicate that at room temperature the magnetic properties of the various rare-earth solute species dissolved in cerium to the extent of 2 a/o have no appreciable effect on the electrical resistivity of the alloys. The slight linear rise in resistivities as a function of atomic number of solute is probably attributable to lattice strains resulting from differences between the atomic sizes of the solvent and solutes. Since in both the γ and β phases the cerium atoms are trivalent,[8] the effect of the lanthanide contraction in the other trivalent rare earths is to cause the greater size mismatch to occur with the heavier rare earth solutes. This would then lead to higher resistivities for those alloys near the lutetium end of the series, as was found experimentally.

Measured resistivities at 4°K are shown in Fig. 1(b). The lower curve represents measurements on specimens cooled rapidly to liquid helium temperature from the annealed state. It might be inferred from this curve that the resistivities of these samples, which were predominantly α phase, is a function of some solute property which relates to a minimum near neodymium or samarium. However, examination of the curves of resistivity as a function of temperature for the various samples heated slowly from 4°K indicated that this was not the case. Instead, it appeared that the resistivity variation as a function of atomic number of solute was due to the different percentages of β phase present in these otherwise α alloys at 4°K. It was possible from examination of the heating curves to make a crude estimate of the amount of β present in the α phase, by observing the magnitude of the resistivity change at the Neél point of the β phase. The smallest discontinuities occurred at about samarium or gadolinium in the series, and the largest at lanthanum and lutetium. Thus, with regard to the "alpha" curve in Fig. 1(b), we conclude that the various amounts of high-resistivity β phase present in the predominantly α-phase specimens may have obscured any possible contributions due to magnetic properties of the rare earth solutes.

The upper curve of Fig. 1(b) represents resistivities of the cerium alloy samples at 4°K after 24 thermal cycles to that low temperature. The departure of this curve from a straight line can largely be attributed to a lack of phase purity. It was found from examination of the resistivity vs. temperature curves of these predominantly β samples that some α phase formed on cooling at low temperatures but reverted to β phase on warming, so that the samples at room temperatures were always in the β form. The amount of α present in these samples at 4°K (as deduced from the resistivity-temperature curves) was greatest at samarium and least at lanthanum and lutetium. Thus the presence of some low-resistivity α phase in the predominantly β samples would, at least in part, account for the shape of the curve.

We think that the resistivities of the predominantly β samples at

4°K can be roughly corrected for α-phase effects, since the percentages of α from sample to sample appeared to be rather small. The corrections would tend to straighten the "beta" line shown, so that a straight line would approximate the corrected data. A straight line suggests that at low temperatures the magnetic properties of the rare-earth solutes in β cerium have no major effect on the electrical resistivities of the alloys. A rise in resistivities toward the heavy end of the series is observed, as was seen at higher temperatures, and may be attributable to size effects. The magnitude of the effect at low temperatures, however, is larger than was found at room temperature (Fig. 1(a)).

We have thus far discussed only the measured values of electrical resistivity as a function of solute species in our attempt to determine the effect of the magnetic properties of the solute atoms on resistivities of the alloys. Of more fundamental significance are the results of an examination of spin-disorder resistivity, since this parameter is not as subject to secondary influences as is measured resistivity. Spin-disorder resistivity is defined here as the difference between the paramagnetic resistivity and the residual resistivity, both extrapolated graphically to 0°K. The paramagnetic resistivities were extrapolated from the linear paramagnetic regions in the resistivity-temperature curves· the residual resistivities were extrapolated from the resistivity data obtained at the lowest temperatures.

Spin-disorder resistivities were thus obtained from the resistivity-temperature plots of the predominantly β samples, which ordered magnetically at ~ 17°K. The parameters used to calculate spin-disorder resistivity, and the results obtained, are shown in Table II. Spin-disorder resistivity as a function of atomic number of solute is shown in Fig. 2. The dip in the curve at samarium is partially due to the presence of a relatively high percentage of α phase, as discussed earlier. Our experimental evidence indicates that the spin-disorder resistivity, if present at all, is lower in α phase than in β. However, a rough correction to remove the effects of the various amounts of alpha present in the β specimens did not change the overall shape of the curve. It

thus appears that the true curve for spin-disorder resistivity as a function of atomic number of solute would have slight dips near the center and at the ends of the series, somewhat reminiscent of the variation of the magnetic parameter L (L+1) across the rare earth series, where L is the total orbital angular momentum. The magnitude of the dips, however, is about the same as that due to experimental scatter. The only trend clearly established in this experiment was a slightly negative slope toward the heavier rare earths.

The present findings show no clear variation of resistivities with any magnetic parameter across the rare earth series. If such a dependence does exist, it is likely that it could be unambiguously detected by the present technique only if a higher percentage of solute were present. Such solute concentrations, however, were not required in the experiments of Mackintosh and Smidt,[5] who added small percentages of heavy rare earths to lutetium and found significant changes in residual resistivities which they correlated with the magnetic parameter $(g-1)^2J(J+1)$. Smidt and Daane,[9] when they alloyed rare earths with other rare earths, found large variations in spin-disorder resistivities and a correlation with the term $(g-1)^2J(J+1)$. Their experiments are not directly comparable with ours, however, since they examined much higher solute concentrations. They also found that the magnetic ordering temperatures varied greatly with alloying content. In the present experiment negligible variations in β-phase Neél temperatures across the rare-earth solute series were found, an observation consistent with the absence of any detectable dependence of resistivity on magnetic parameters.

The same cerium-rich compositions discussed here were found by Gschneidner *et al*[4] to show a solute spin-dependent effect on the $\gamma \rightarrow \alpha$ transformation temperatures. It is not clear why a similar effect was not observed in the present electrical resistivity data if the conduction electrons are involved in the coupling of the 4f electrons.

The negative slope seen in the plot of spin-disorder resistivity as a function of increasing solute atomic number (Fig. 2) is rather minor. It may be related to the observation[10] that the energetically deep 4f

shells in the heavier rare earths are highly localized and do not interact strongly, whereas the energy levels for the 4f electrons in the lighter rare earths are closer to those for the 5d 6s states, and thus may interact to some extent. From this view, the magnetic interaction of solvent and solute atoms by the Friedel-Rocher mechanism of virtual bound states[10,11] might be expected to be less with heavy rare earth solutes, and thus decrease spin-disorder resistivity when these elements are present in cerium. It is also possible that the negative slope in Fig. 2 may be due to changes in band structure or Fermi level as alloying elements are added to cerium.

SUMMARY

Two atomic percent of the various trivalent rare earths were dissolved in cerium, and the electrical resistivities of these dilute binary alloyw determined in the range 1.5 to 297°K. Resistivities are reported for: predominantly γ phase at 297°K, β phase at 297°K, predominantly α phase at 4°K, and predominantly β phase at 4°K.

Resistivities at 297°K for both γ and β phases were found to be a linear function of atomic number of solute, with a slight increase toward the heavy rare earths being attributed to atomic size effects.

Resistivities for predominantly α-phase samples at 4°K were found to be influenced significantly by the percentages of β phase retained on cooling. β-phase resistivities at 4°K were also affected by small amounts of α phase present.

Spin-disorder resistivities were determined for the predominantly β samples and were found not to reflect the influence of solute magnetic parameters that had been suggested by the work of others. A slight downward trend in spin-disorder resistivities was detected with increasing atomic number of solute, and is considered in terms of a virtual bound state model.

ACKNOWLEDGMENTS

The authors wish to express their appreciation to the following: Dorothy Garinger, for assisting in the performance of the laboratory

experiments; V. O. Struebing and James Shore, for making the alloys; Donald Braid, for design of the cyrogenic apparatus; James Deal and Verner Rexroth, for design of the electronic circuitry; and Ivan Cherry and Bertha Fagan, for planning and executing the computer program.

REFERENCES

1. K. A. Gschneidner, Rare Earth Alloys, D. Van Nostrand, Princeton (1961).

2. C. J. McHargue and H. L. Yakel, Jr., Acta Met. 8, 637 (1960).

3. M. K. Wilkinson, H. R. Child, C. J. McHargue, W. C. Koehler, and E. O. Wollan, Phys. Rev. 122, 1409 (1961).

4. K. A. Gschneidner, Jr., R. O. Elliott, and R. R. McDonald, J. Phys. Chem. Solids 23, 1201 (1962).

5. A. R. Mackintosh and F. A. Smidt, Jr., Phys. Letters 2, 107 (1962).

6. K. A. Gschneidner, Jr., R. O. Elliott, and R. R. McDonald, J. Phys. Chem. Solids 23, 555 (1962).

7. F. K. Harris, Electrical Measurements, p. 176, John Wiley and Sons, New York (1952).

8. K. A. Gschneidner, Jr., J. Less-Common Metals 5, 374 (1963).

9. F. A. Smidt, Jr. and A. H. Daane, J. Phys. Chem. Solids 24, 361 (1963).

10. Y. A. Rocher, Advan. Phys. 11, 233 (1962).

11. J. Friedel, J. Physique et le Radium 23, 692 (1962).

Table I. Room-temperature gamma and beta phase densities of cerium containing 2 a/o of various other rare earths. (Density determination by an immersion method.)

Solute	La	Pr	Nd	Sm	Gd	Tb	Dy	Ho	Er	Tm	Lu
γ-phase density* (g/cm^3)	6.73	6.75	6.76	6.76	6.77	6.77	6.78	6.78	[6.77]	[6.78]	[6.77]
β-phase density (g/cm^3)	6.67	6.69	6.70	6.71	6.71	6.72	6.72	6.72	6.73	6.73	6.74
Density diff.	0.06	0.06	0.06	0.05	0.06	0.05	0.06	0.06	0.04	0.05	0.03

* Brackets indicate uncertainty in phase purity.

Table II. Resistivities of cerium, predominantly beta phase, containing 2 a/o of various other rare earths. (Units of ρ are μΩ-cm.)

Solute	La	Pr	Nd	Sm	Gd	Tb	Dy	Ho	Er	Tm	Lu
ρ at 4°K	16.8	15.0	16.6	19.0	24.6	25.0	24.4	27.5	24.0	26.2	30.1
Paramagnetic ρ extrap. to 0°K	49.8	47.7	47.8	46.9	52.3	54.0	52.7	56.3	53.2	55.5	57.0
Residual ρ extrap. to 0°K	15.1	12.9	14.4	17.0	22.5	22.9	22.6	25.6	22.1	24.4	28.2
Spin-disorder ρ* at 0°K	34.7	34.8	33.4	29.9	29.8	31.1	30.1	30.7	31.1	31.1	28.8

* The spin-disorder resistivity was obtained by subtracting the residual resistivity from the paramagnetic resistivity, both extrapolated to 0°K.

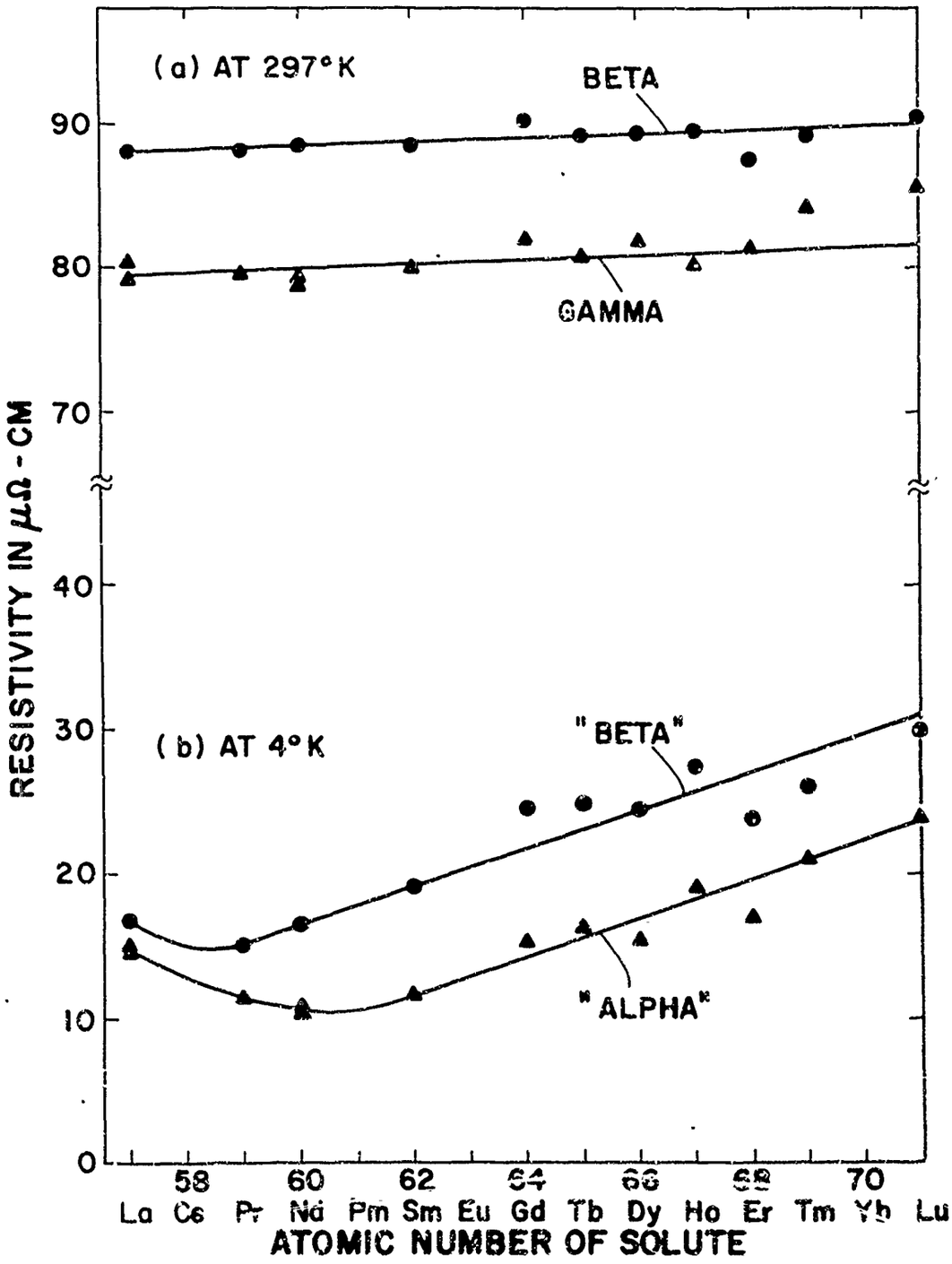

Fig. 1. Resistivities of cerium containing 2 a/o additions of various other rare earths. Quotation marks around the words alpha and beta indicate uncertainty in the phase purities of these alloys.

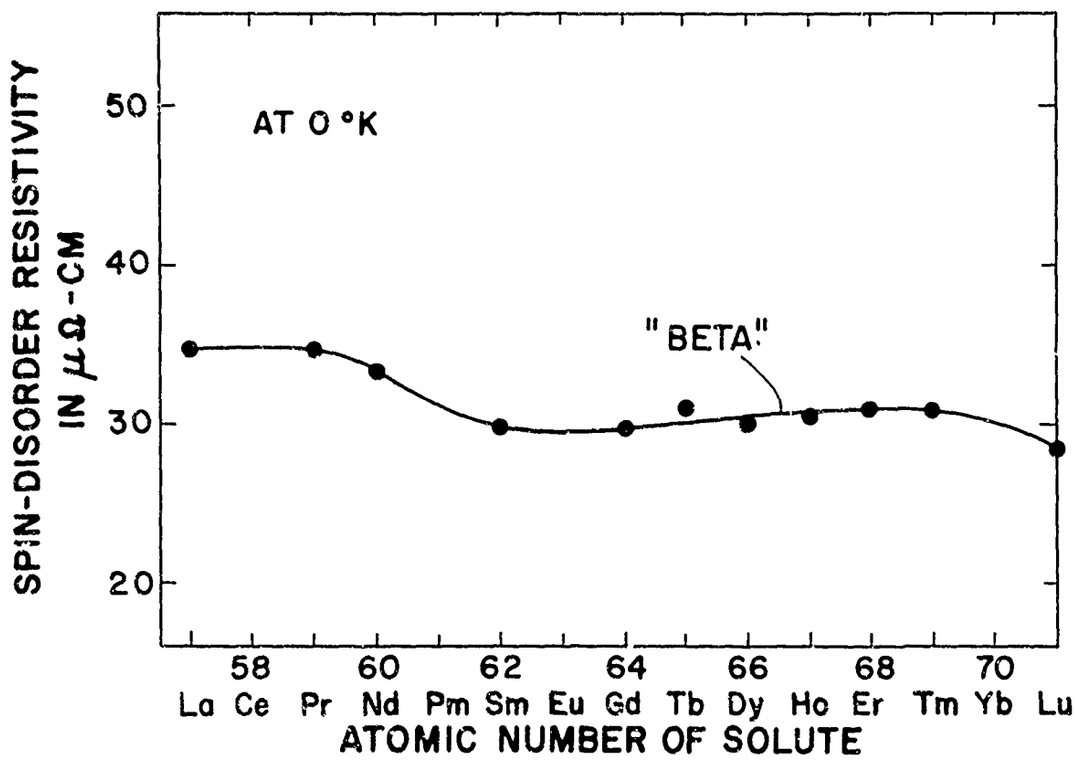

Fig. 2. Spin-disorder resistivity of beta cerium (containing 2 a/o additions of various other rare earths) as a function of the atomic number of solute. Quotation marks around the word beta indicate an uncertainty in the phase purity of these alloys.

SPIN DEPENDENCE OF THE ELECTRICAL RESISTIVITIES OF GADOLINIUM ALLOYS*

C. W. Chen

Westinghouse Research Laboratories
Pittsburgh, Pennsylvania 15235

ABSTRACT

The electrical resistivities of various intra-rare-earth alloys of gadolinium at 4.2°, 77°, and 298°K are discussed with respect to the theory. Two spin effects are shown in the scattering of the conduction electrons.

*This research was supported by the Advanced Research Projects Agency, Director for Materials Sciences and was technically monitored by the Air Force Office of Scientific Research under Contract AF49(638)-1245.

We have determined the resistivities of various gadolinium alloys at 4.2°, 77°, and 298°K. The electrical data permit a critical study of the scattering of the conduction electrons. The following conclusions are particularly important and thought to be valid for all intra-rare-earth alloys having localized magnetic moments.

(1) The increases in the residual resistivity of Gd are strongly spin dependent. The impurity scattering of electrons is due predominantly to a spin inhomogeneity effect.

(2) At temperatures above the Curie point, the spin-disorder resistance is so preponderant that the impurity effect on scattering becomes obscure and the intrinsic effect of spin disorder dominates the scattering.

(3) If the scattering caused by the two spin effects just stated can indeed be suitably treated by the Born approximation method, as has been done by Dekker,[1] the spin-disorder resistivity of Gd, ρ_{sd}, above the Curie point would be much larger than the value obtained by extrapolation.[2,3] Such a discrepancy reflects an inadequacy of the present theory.

We chose Gd as the base metal for its simple $^{8}S_{7/2}$ ground state. The single magnetic transition and its Curie temperature ($\theta_c = 289^{\circ}$K) were also considered to be desirable. The solute elements examined include La and all rare earths except Pm, Eu, and Yb.

At 4.2° and 77°K, all solutes were observed to increase the resistivity of Gd according to the Nordheim approximation. By plotting $\Delta\rho/(1-c)$ *vs.* c, we can evaluate the atomic resistivity increase caused

by impurity in terms of $\Delta\rho/c(1-c)$, where $\Delta\rho = \rho_{alloy} - \rho_{Gd}$ and c is the atomic concentration of the solute. In Fig. 1, the values of $\Delta\rho/c(1-c)$ deduced from the data at $4.2^{\circ}K$ are plotted against S^2, where S has the value of the difference between the atomic numbers of Gd and the solute element. It is seen that all experimental points except that of Ce fall upon two straight lines parallel to each other within the experimental error. Hence we obtain an empirical formula of the form

$$\Delta\rho = c(1-c)(A + BS^2) \qquad (1)$$

with apparently different A values but the same B value for the light and heavy lanthanides. Equation (1) is also valid at $77^{\circ}K$, but at $298^{\circ}K$, nearly all $\Delta\rho$ disappeared as the alloys showed resistivities within $\pm$ 2% of the value (135 $\mu\Omega$-cm) for pure Gd.

The results at $298^{\circ}K$ point out the difference between the Gd and certain noble metal alloys[4] and imply a strong spin dependence of the scattering mechanism leading to $\Delta\rho$. The former conclusion is also supported by the fact that all rare earth ions under consideration (except Ce, see Fig. 1) have equivalent electron configurations leading to a pseudotrivalence.[5] Therefore the Gd alloys are expected to show little resistance due to electrostatic scattering, as is evidenced by the small intercepts of the best-fit lines in Fig. 1 and BS^2 is to be identified with the resistivity due to exchange scattering with S becoming the difference between the spins of Gd and the solute ions.

This interpretation of Eq. (1) is in agreement with Dekker's analysis for the case that the coupling constant G of the indirect spin interaction between the conduction electrons and the magnetic shells is invariant with the spin operator of the magnetic ions $\underline{S}$. The Hamiltonian of the interaction is written as $-2G\delta(r_i-R_j)\underline{s}_i\cdot\underline{S}_j$, where $\underline{s}_i$ is the spin operator of a conduction electron at r_i. The question as to whether G is constant or not has been discussed by Liu[6] and Watson and Freeman.[7]

Although the indirect spin interaction is essential in the consideration of the exchange scattering, the interaction per se does not cause the scattering. Thus Kasuya[8] has predicted a zero resistivity for perfectly pure Gd at $0^{\circ}K$. The real cause of the exchange scattering is the inhomogeneity of the spin lattice produced by the solute atoms and the scattering occurs only at the solute sites where the perturbations are centered. These points have been overlooked by some authors.[3]

It should also be cited that the simple relation $\Delta\rho \sim S^2$ has never been observed in the alloys of Fe, Co, and Ni. This is probably because the wave functions of the 3d electrons are not so localized as those of the 4f electrons. Also, in the 3d transition metal alloys, the Coulomb scattering potentials are not necessarily small and complications arise such as the resonance scattering caused by the virtual states.[9]

To illustrate the difficulty encountered in the reconciliation of the observed $\Delta\rho$ in the Gd alloys with the spin-disorder

resistivity, we recall that both Dekker and de Gennes and Friedel[10] have arrived at a $S'(S'+1)$ dependence of ρ_{sd} for Gd, where S' is the atomic spin of Gd. Further, from Dekker's analysis, an expression may be obtained comparing ρ_{sd} with the resistivity increase caused by the spin inhomogeneity effect, ρ_{si}, in a Gd alloy at $0^{\circ}K$

$$\frac{\rho_{sd}(T \gg \theta_c)}{\rho_{si}(0)} = \frac{S'(S'+1)}{cS^2} \qquad (2)$$

Since $\rho_{si}(0)$ may be estimated from the results shown in Fig. 1, ρ_{sd} can be calculated from Eq. (2). Taking $Gd_{97}La_3$ as a typical example, $\Delta\rho$ at $4.2^{\circ}K$ is 11 $\mu\Omega$-cm and $\rho_{si}(0)$ is approximately 10 $\mu\Omega$-cm. With $S' = 7/2$, ρ_{sd} is calculated to be 430 $\mu\Omega$-cm, as compared with the extrapolated value of 111^2-120^3 $\mu\Omega$-cm.

This large discrepancy between the calculated and extrapolated values of ρ_{sd} demands a careful re-examination of the theory. One possible explanation might be that the scattering involving spin flip is merely a mathematical consequence induced by the spin step-up and step-down operators components, $\frac{1}{2}(s_+S_- + s_-S_+)$, of the $\underline{s}\cdot\underline{S}$ coupling. In reality, the paramagnetic state may show short-range order of the spins, thereby allowing only the elastic scattering due to the s_zS_z component of the coupling in the temperature range from which the extrapolated value of ρ_{sd} has been obtained. If this is true, ρ_{sd} would depend upon $\overline{S'^2}$, instead of $S'(S'+1)$. By assuming equal probability for all possible values of S'^2, we have $\overline{S'^2} = 21/4$ and the calculated value of ρ_{sd} is 143 $\mu\Omega$-cm. The discrepancy would then

be reduced to a satisfactory level. To test this possibility, resistance measurements were conducted on a Gd sample at elevated temperatures. The resistivity of Gd was observed to increase parabolically with temperature from 300°K to a value of 190 microhm-cm at 1030°K, and remain almost unchanged between 1030° and 1250°K. There was no indication, at least up to 1250°K, that the resistivity of Gd would rise sharply to reach the predicted value of ρ_{sd} including spin flip.

The author is indebted to Dr. P.G. Klemens for his valuable contribution to the discovery of the discrepancy in the calculation of ρ_{sd} and comments on the manuscript and to Dr. W.J. Carr, Jr. for stimulating discussion.

References

1. A.J. Dekker, Phys. Stat. Sol., 7, 241 (1964); J. Appl. Phys. 36, 906 (1965).
2. J. Hennephof, Phys. Letters, 11, 273 (1964).
3. R.J. Weiss and A.S. Marotta, J. Phys. Chem. Solids, 9, 302 (1959).
4. J.O. Linde, Ann. Physik, 15, 219 (1932).
5. B.R. Judd and I. Lindgren, Phys. Rev. 122, 1802 (1961).
6. S.H. Liu, Phys. Rev., 123, 470 (1961).
7. R.E. Watson and A.J. Freeman, Phys. Rev. Letters, 14, 695 (1965).
8. T. Kasuya, Progr. Theor. Phys. (Kyoto), 22, 227 (1957).
9. C.W. Chen, Phys. Letters, 7, 16 (1963).
10. P.G. de Gennes and J. Friedel, J. Phys. Chem. Solids, 4, 71 (1958).

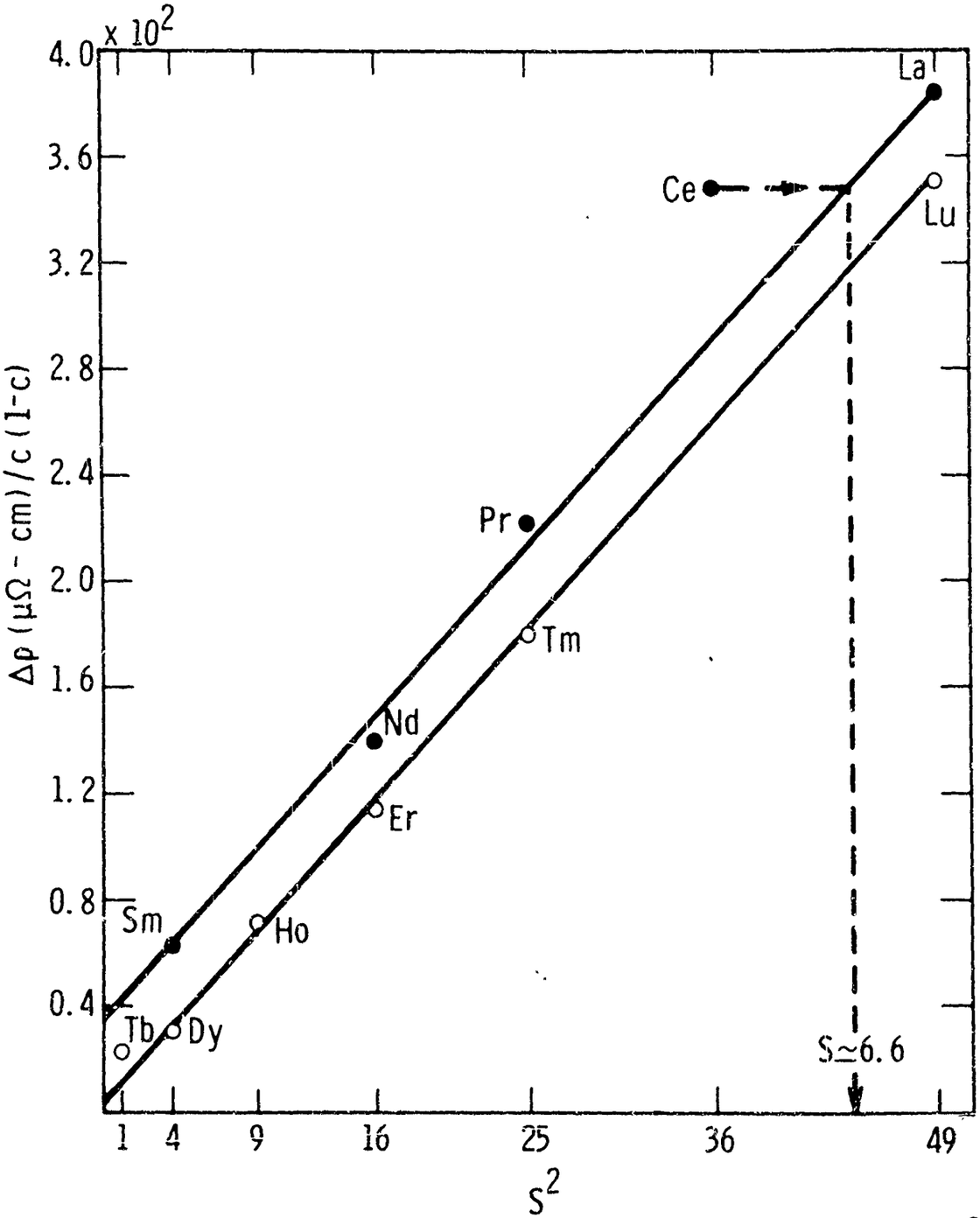

Fig. 1—A linear relationship is seen between $\Delta\rho/c(1-c)$ and S^2 at 4.2°K for both light (La-Sm) and heavy (Tb-Lu) rare earth solutes in Gd. The dashed lines indicate a possible explanation of the large deviation from the linear relationship of the Ce point. Instead of 6, S is approximately 6.6, corresponding to 60% of the Ce ions in the tetravalent state.

MAGNETIC TRANSFORMATION IN HEAVY RARE-EARTH ALLOYS WITH EACH OTHER

R. M. Bozorth and R. J. Gambino

IBM Watson Research Center
Yorktown Heights, New York

ABSTRACT

We have measured the Curie (T_C) and Néel (T_N) points of the binary intra-rare-earth alloys Gd-Lu, Dy-Ho, Dy-Tm, Er-Tm, and Tm-Lu, in addition to those previously reported (Atlantic City, Nottingham). There are maxima in the Curie point vs composition curves for Ho-Er, Ho-Tm, and Er-Tm, minima for Dy-Tm and Ho-Tm, when the average concentration of 4f electrons is near 10.5. The Tm-Lu alloys are ferromagnetic when Tm-rich, and distilled Tm has a Curie point, Néel point, and intermediate transformation point. The Lu-rich alloys are all non-ferromagnetic in low fields and some become ferromagnetic at a critical field, when they have sharply increased susceptibility with onset of hysteresis. Representative data for various alloy systems are shown to deviate only slightly from a straight line when plotted against the 2/3 power of the average de Gennes factor, as discussed by Koehler.

METHODS

Materials were prepared by arc melting and annealing in closed containers and then tested for homogeneity as previously described.[1,2] The anneal was normally 1050°C but alloys containing Tm were annealed at 850°C. The distilled Tm was prepared by sublimation in a vacuum of 10^{-6} mm at 1500°C.

Magnetic measurements were made with the pendulum magnetometer previously described.[3] Although several methods were used for determining the Curie point (T_C), the method generally employed depends on finding the point of inflection of the moment (σ) vs temperature (T) curves for two or three relatively low fields and extrapolating these points to zero field. Normally the point of inflection is determined visually but it is possibly also to plot $\Delta\sigma/\Delta T$, using the $\Delta\sigma$ and ΔT between neighboring points on the σ, T curve, and so finding the temperature of maximum slope. This "inflection" method as applied to Ho and Er gives the same values of T_C as those previously reported in the literature, and Dr. R. Joenk has shown that the method is consistent with molecular field theory. In the case of Tm the inflection point comes at 25°K, 3° above the temperature previously reported,[4] and will be discussed below.

The Néel points are readily detected as sharp maxima in the σ, T curves, extrapolated to zero field. The difference in the character of the singularity in the σ, T curve at T_C and T_N is especially apparent in the Gd-rich alloys, in some of which T_C and T_N coincide and are properly considered to be Curie points, whereas other alloys show on cooling first the sharp peak of a Neel point and at lower temperatures these may or may not show a true Curie point.

RESULTS

In Figure 1 we plot T_C and T_N against the average number, n,

of 4f electrons per atom of alloy. As previously noted T_N is nearly a universal function of n as long as the n's of the component elements are not too different. For Gd-Lu, however, there is a large departure from most of the other systems such as Ho-Er. Following Koehler et al.[6] this departure disappears when T_N is plotted against $\bar{G}^{2/3}$, where $\bar{G}$ is the average of the de Gennes[5] factors:

$$G = (g-1)^2 J(J+1) \quad , \qquad \bar{G} = c_1 G_1 + c_2 G_2 \quad ,$$

c_1 and c_2 being the atomic fractions for which $G = G_1$ and G_2. Figure 2 shows such a plot for many of our alloys and also for a number reported by the group at Oak Ridge National Laboratory.[7] The departure of some of the points from the straight line appears to be well outside the experimental error; recently we have confirmed the determination of T_N for one of the Gd-Er alloys[1] from the presumed best line. There thus appears to be some deviation from the empirical 2/3 power relation not accounted for by experimental error or impurities.

Data used in the determination of the Néel and Curie points of two Tm-Lu alloys are shown as examples in Figure 3. T_C for $Tm_{0.6}Lu_{0.4}$, if it exists at all, is below 2°K, but evidence of ferromagnetism, or of some change in structure, is shown by the change in slope of the magnetization curves of Figure 4.

The values of T_C plotted in Figure 1 are distinctly characteristic of each alloy system. Greater departures from linearity, in the curves joining two elements, are found in the middle of the diagram near the concentration of 4f electrons of 10.5, known[8] to be the point at which the 4f electron cloud changes from prolate to oblate and as a result the crystal anisotropy[9] and magnetostriction[10] change in sign. The fractional increase in T_C of the alloy as compared to that of the component elements is high in the Ho-Er alloys(35°, cf. 20°) and even

higher in the Er-Tm alloys (43°, cf. 20° and 25°). On the contrary T_C is depressed by alloying Dy and Tm and T_C is then lowered from 85° and 25° to 7°K.

There is special interest in the element Tm. Previous measurements, based on the existence of hysteresis, indicated that $T_C = 22°$. Recently we have measured the loops of material obtained from the manufacturer and annealed, and the same material as distilled and analyzed, at 1.25°K with $H_{max} = 25$ kOe. As may be seen in Figure 5 the former material showed hysteresis with a coercive force of about 4 kOe and a sharp increase in σ as H exceeded 20 kOe. Spectroscopic analysis showed 0.6 at. % Ta and 0.4 at. % O. On the contrary the distilled material, containing 0.02 at. % Ta and 0.4 at. % O, showed no such increase up to 25 kOe. Measurements by T. R. McGuire in fields to 50 kOe, however, showed a sharp increase in σ beginning at about 30 kOe and still rising rapidly at 50 kOe, when the moment was about 2.5 Bohr units per atom. Apparently the 4, 3, 4, 3 structure found by neutron diffraction[11] in zero field is broken down in high fields. (The theoretical gJ is 7.0.)

The point of inflection of the σ, T curve for Tm is found to be 25°K, as extrapolated to H = 0. The slope of the curve (Figure 6) was determined for distilled material with some accuracy by measuring both $\Delta\sigma$ and ΔT between neighboring points taken for H = 2 kOe. A plot of the (negative) slope (Figure 7) shows a well-defined maximum at 26°K. At 33°K a sharp decrease in the σ, T curve is observed such that the slope then rises suddenly to a new higher maximum, indicative of a departure from the 4, 3, 4, 3 arrangement and the formation of a new magnetic structure. Sharp decreases of this kind were found for three different specimens of Tm of different origin.

The Curie points of Tm-rich Tm-Lu alloys decrease rapidly to zero, and are not ferromagnetic above a concentration of about 30% Lu.

Néel points were determined to about 90% Lu and follow the $\overline{G}^{2/3}$ law with some accuracy (see Figure 2).

References

1. R. M. Bozorth and R. Gambino, Proc. Intern. Conf. on Magnetism, Nottingham (1964), in press. (p. 263).
2. R. M. Bozorth and J. C. Suits, J. Appl. Phys. 35, 1039 (1964).
3. Bozorth, Williams, and Walsh, Phys. Rev. 103, 572 (1956).
4. D. D. Davis and R. M. Bozorth, Phys. Rev. 118, 1543 (1960).
5. P. G. de Gennes, J. phys. radium 23, 510 (1962).
6. Koehler, Wollan, Child, and Cable, Rare-Earth Research, (K. S. Vorres, Ed.) Gordon and Breach, New York, p. 199 (1964). See also Weinstein, Craig, and Wallace, J. Appl. Phys. 34, 1354 (1963), for the use of the 3/2 power law of T_N vs composition of solid solutions with yttrium.
7. Summarized by H. R. Child, Thesis, University of Tennessee (1965).
8. K. W. H. Stevens, Proc. Phys. Soc. 65, 209 (1952).
9. R. J. Elliott, Phys. Rev. 124, 346 (1961).
10. Tsuya, Clark, and Bozorth, Proc. Intern. Conf. on Magnetism, Nottingham (1964), in press.
11. Koehler, Cable, Wollan, and Wilkinson, Phys. Rev. 126, 1672 (1962).

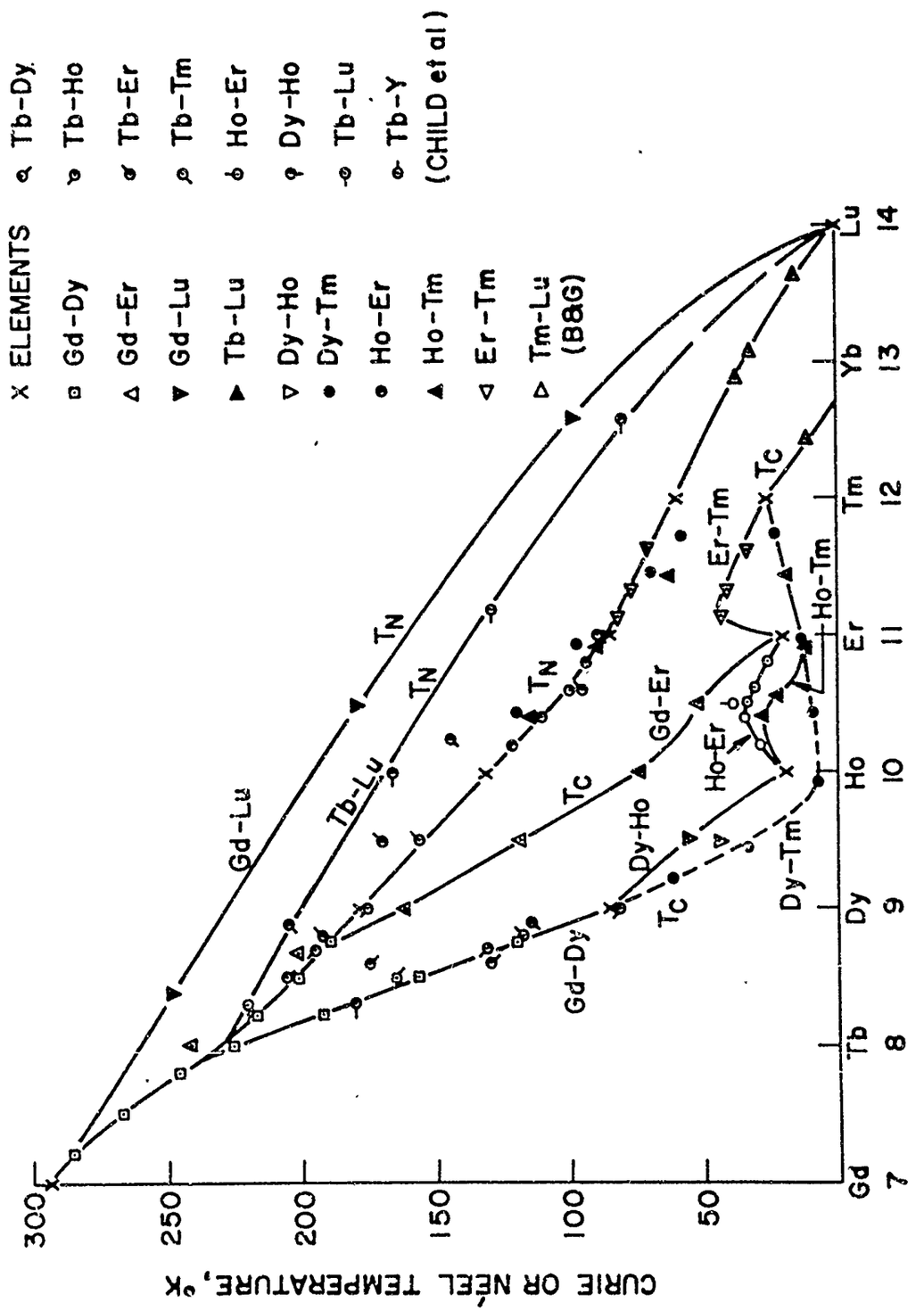

Fig. 1. Curie and Néel points of some binary alloys.

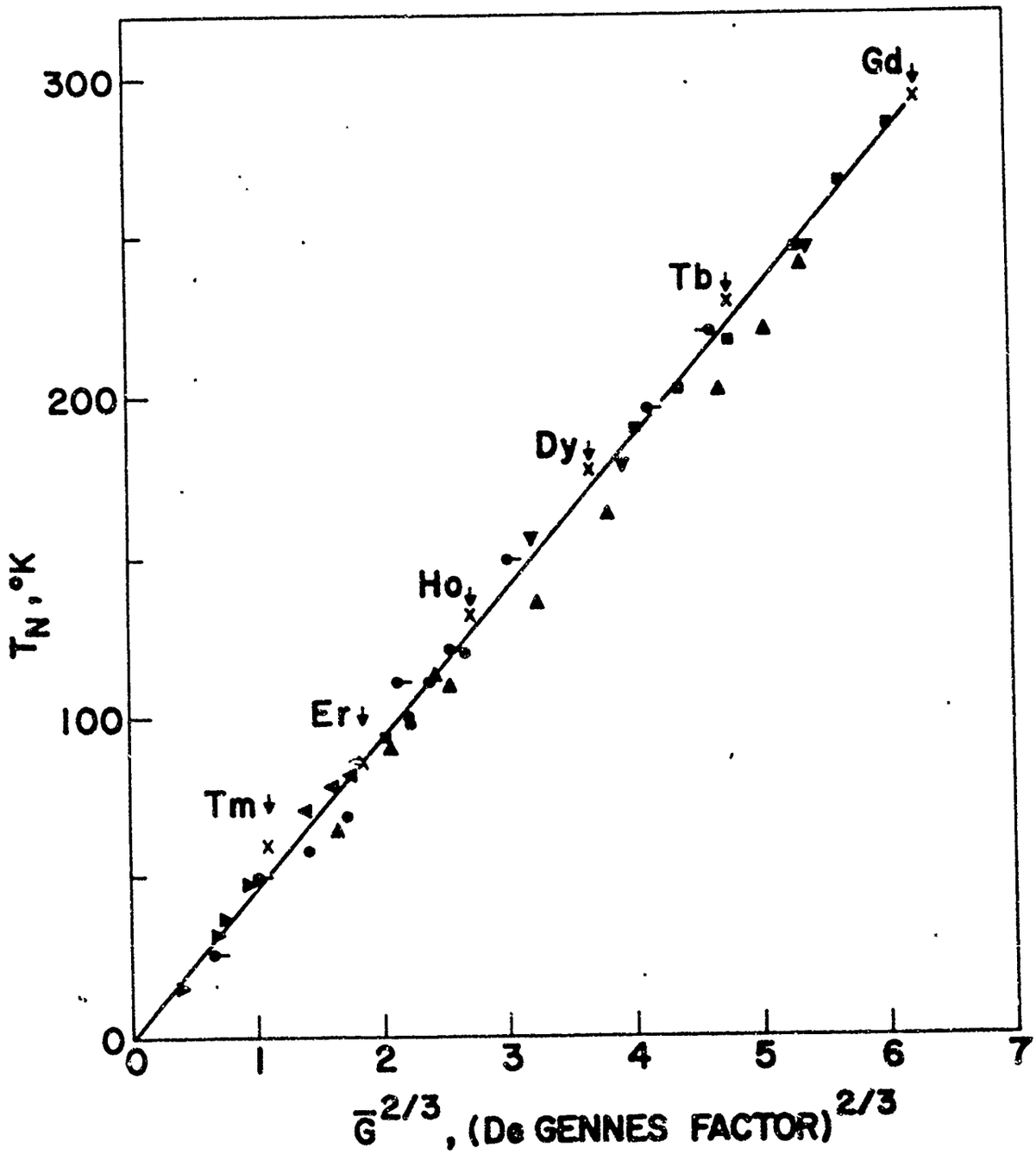

Fig. 2. Néel points of heavy elements and some representative alloys. Symbols of Fig. 1 apply.

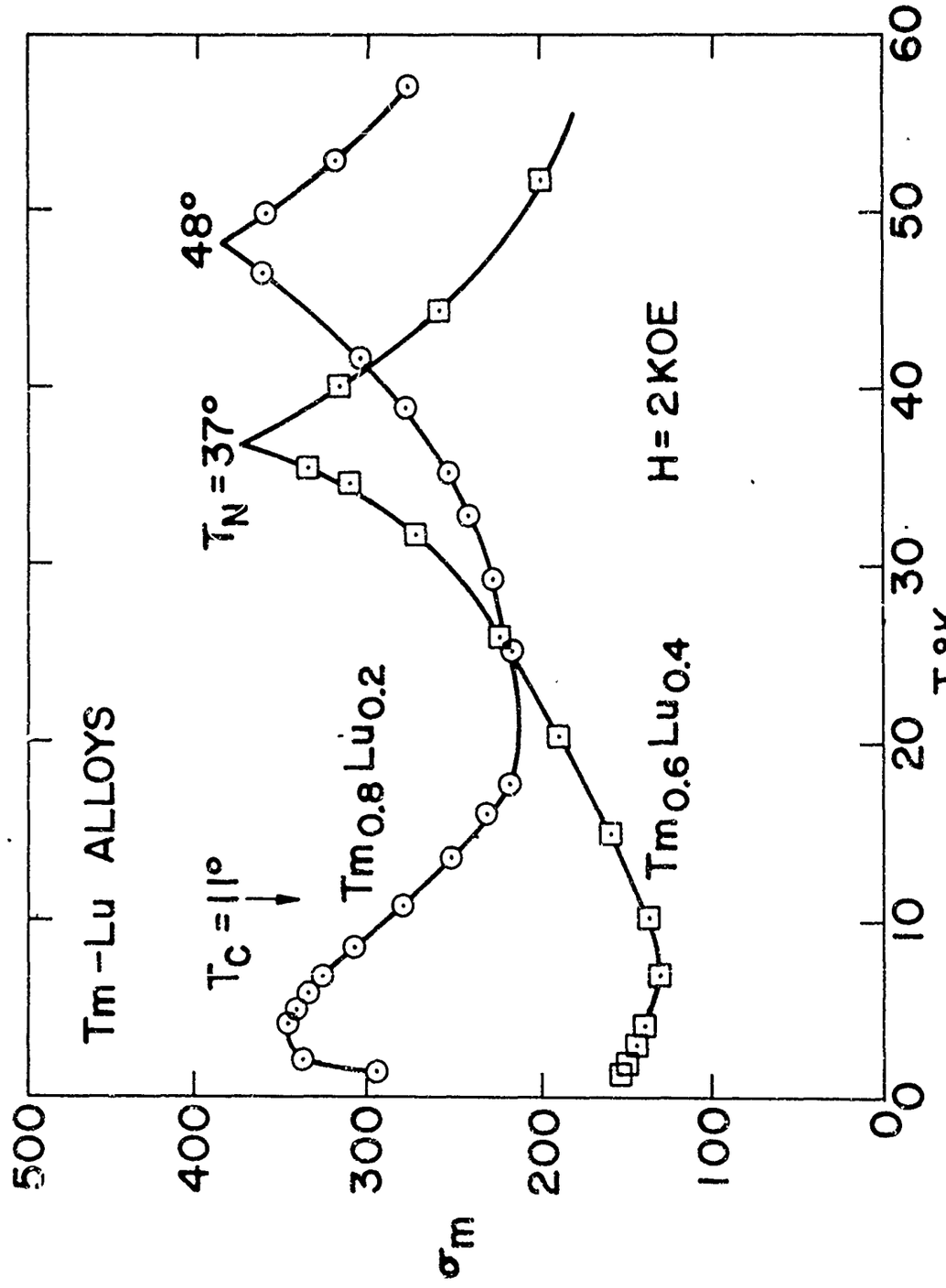

Fig. 3. Data used for T_C and T_N for $Tm_{0.8}Lu_{0.2}$, T_N for $Tm_{0.6}Lu_{0.4}$.

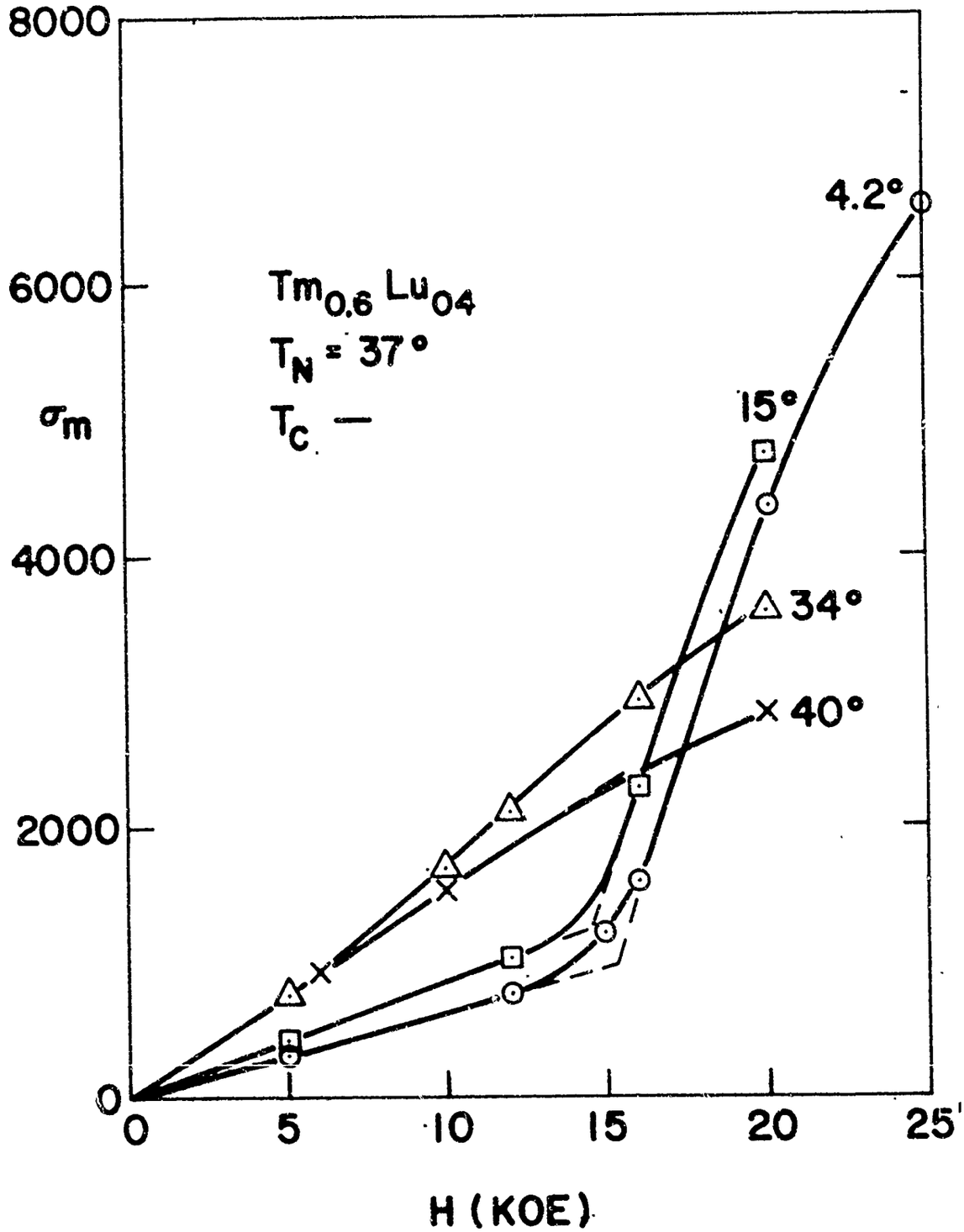

Fig. 4. Magnetization curves of $Tm_{0.6}Lu_{0.4}$, showing sudden increase in σ_m above H = 15 kOe.

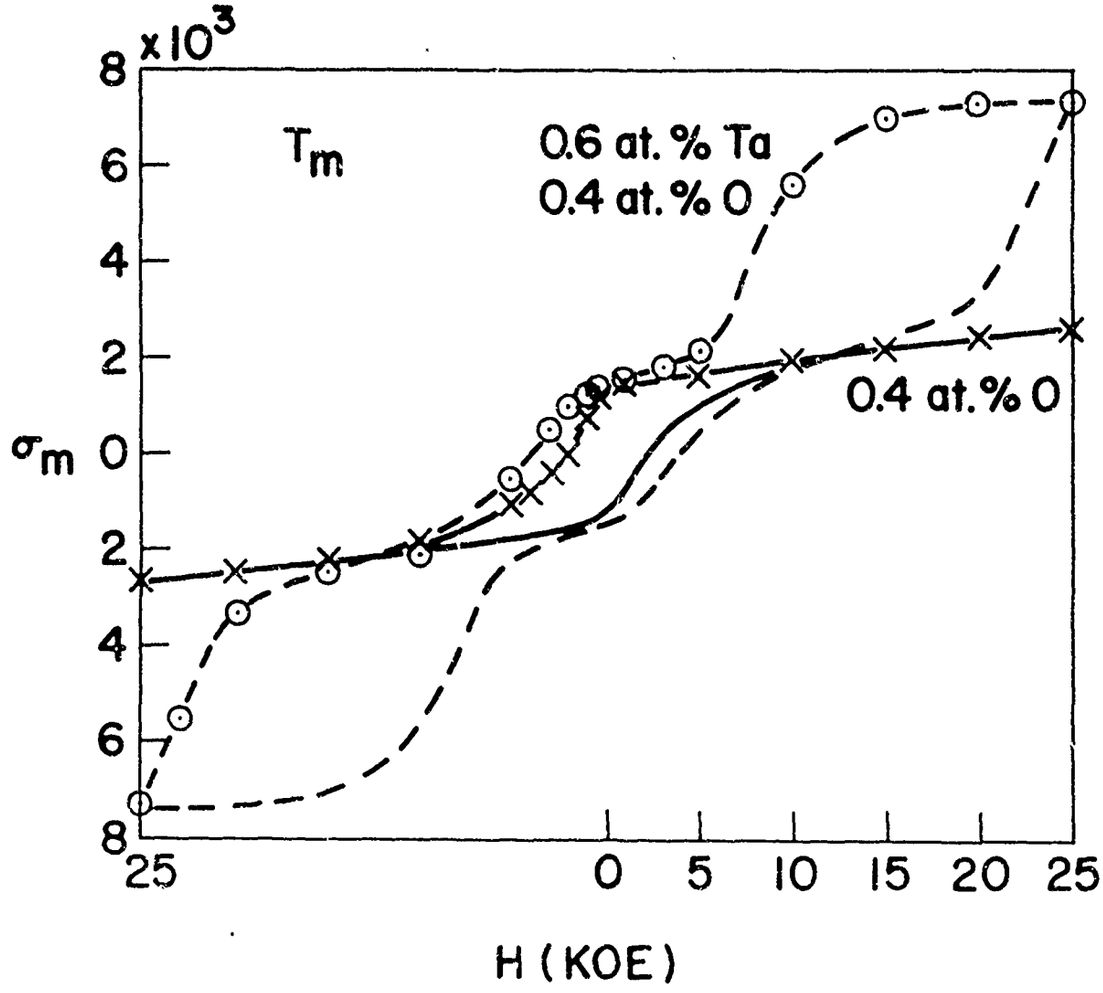

Fig. 5. Hysteresis loops for Tm specimens as received and annealed, and as distilled.

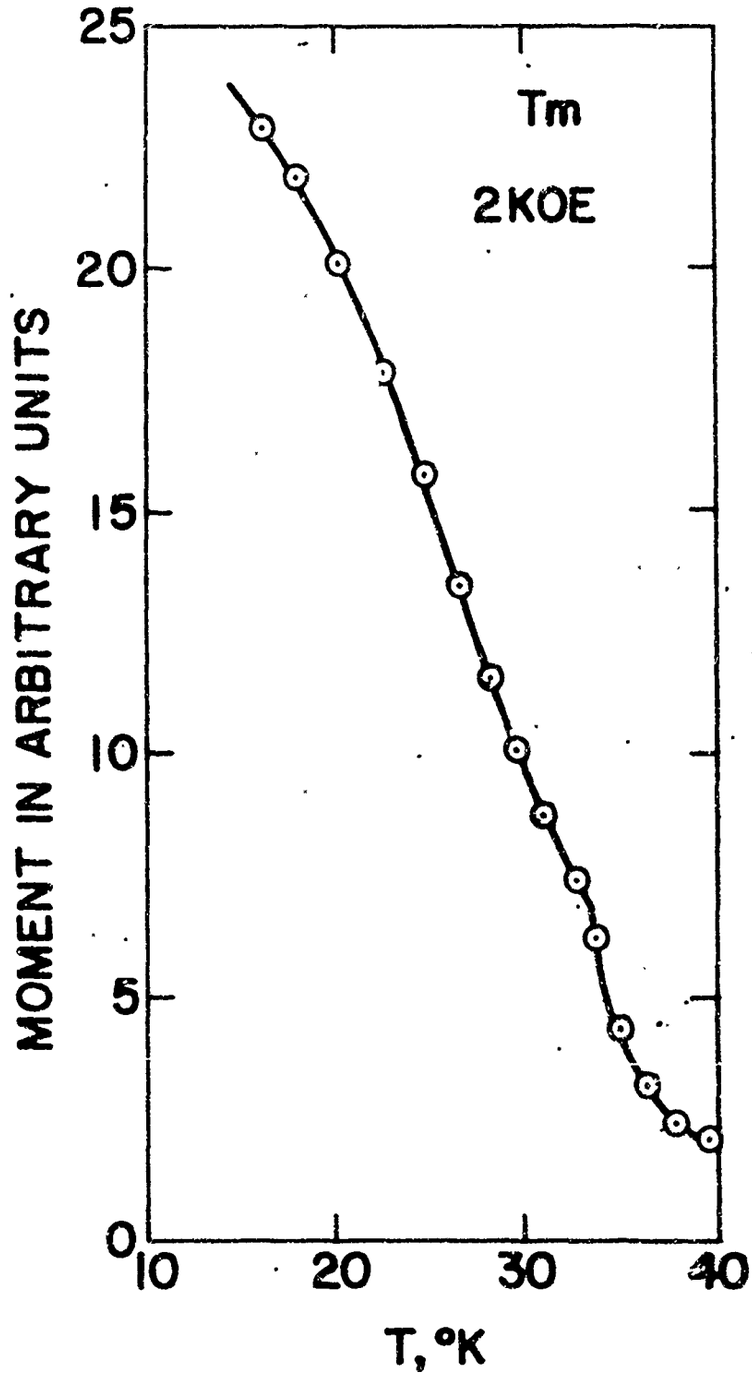

Fig. 6. Moment vs T curve of distilled thulium, for H = 2 kOe.

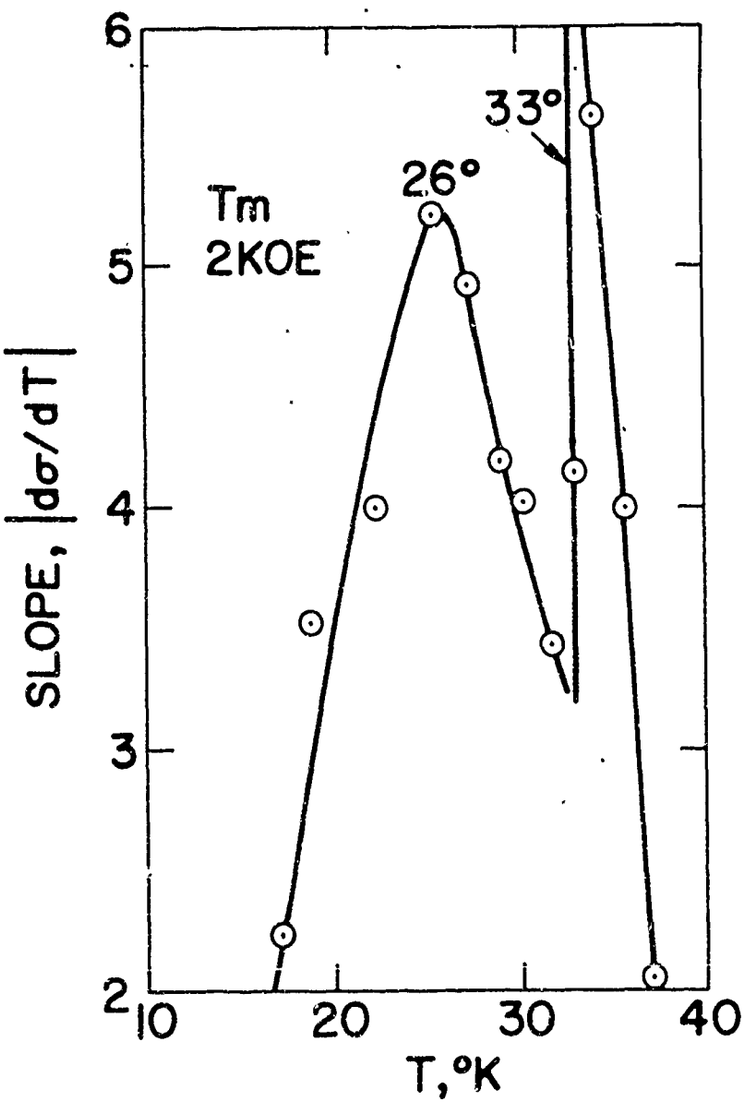

Fig. 7. Slope of curve of Fig. 6, showing maximum at point of inflection, and discontinuity at 33°K.

MAGNETIC PROPERTIES OF RARE EARTH-THORIUM ALLOYS†

† Research sponsored by the U. S. A. E. C. under contract with the Union Carbide Corporation.

W. C. Koehler, H. R. Child and J. W. Cable

Oak Ridge National Laboratory
Oak Ridge, Tennessee

ABSTRACT

Neutron diffraction studies have been carried out on a number of alloys of thorium with the heavy rare earth metals Tb, Ho, and Er as part of an investigation of the nature of the exchange interaction in these materials. At room temperature, and below, the heavy rare earths in question crystallize in the simple hexagonal close packed structure; thorium, in the cubic close packed structure. The interatomic distances in thorium are intermediate between those in Dy and Ho, and relatively wide regions of solid solution have been observed. Alloys containing more than about 80 a/o rare earth are found in the hcp structure, and those with less than about 50 a/o are found in the ccp arrangement. The three outer electrons of the rare earth metals ($5d^1 6s^2$) are presumed to form conduction bands and it is generally accepted that magnetic coupling in the rare earth metals occurs via an indirect interaction involving a polarization of the conduction electrons. Thorium, a tetravalent diluent (outer electron configuration $6d^2 7s^2$) provides a means of changing the effective number of conduction electrons on alloying of the rare earths. In contrast to the effect of trivalent yttrium and lutetium as diluents, small additions of thorium tend to stabilize the ferromagnetic state in the hcp structure. For example, the alloy 10Th-90Ho transforms spontaneously from the helical to the ferromagnetic state and in the alloy 20Th-80Ho the helical configuration was not detected. In the Th-rich region alloys 20Tb-80Th, and 30Tb-70Th have so far been studied. Both of these exhibit diffraction patterns characteristic of short range antiferromagnetic ordering at 4.2°K.

Attempts at correlation of these results with the Ruderman-Kittel-Kasuya-Yosida theory have been made but with indifferent success.

PARAMAGNETIC STUDIES OF HOLMIUM BY NEUTRON TOTAL CROSS SECTION MEASUREMENTS

Marieta Mattos

Instituto de Energia Atômica
São Paulo, Brasil

ABSTRACT

The total neutron cross section for holmium was measured for neutron wavelengths between 0.20 and 9.00 Angstroms. The IEA crystal spectrometer was used together with a mechanical velocity selector to eliminate higher order reflections from the crystal. Powder samples of Ho_2O_3 were prepared in high purity, taking particular care to eliminate contamination by the rare earths of high neutron cross section. Although paramagnetic form factors are usually determined by differential cross section measurements with one neutron wavelength, accurate total cross section measurements for a wide range of known wavelengths give definite information on the radius of the 4 f electron orbits. Our measurements indicate a radius different from the one used by Blume, Freeman and Watson, who calculated the form factor assuming hydrogenic wave functions. The possible choice of different screening constant will be discussed.

PARAMAGNETIC STUDIES OF HOLMIUM BY NEUTRON TOTAL CROSS SECTION MEASUREMENTS

by

Marieta C. Mattos

Nuclear Physics Division
Instituto de Energia Atômica
São Paulo - Brasil

PUBLICAÇÃO IEA Nº 99
August, 1965

To be presented at the "5th Rare Earth Research Conference", promoted by the Institute for Atomic Research , Ames, Iowa, USA., August, 1965.

Comissão Nacional de Energia Nuclear

Presidente: Prof. Luiz Cintra do Prado

Universidade de São Paulo

Reitor: Prof. Luiz Antonio da Gama e Silva

Instituto de Energia Atômica

Diretor: Prof. Rômulo Ribeiro Pieroni

Conselho Técnico-Científico do IEA

Prof. José Moura Gonçalves)
Prof. Walter Borzani) pela USP
Prof. Rui Ribeiro Franco)
Prof. Theodoreto H.I. de Arruda Souto) pela CNEN

Divisões Didático-Científicas:

Div. de Física Nuclear: Prof. Marcello D.S. Santos

Div. de Engenharia de Reatores: Prof. Tharcisio D.S. Santos

Div. de Ensino e Formação: Prof. Luiz Cintra do Prado (licenciado)

Div. de Radioquímica: Prof. Fausto Walter de Lima

Div. de Radiobiologia: Prof. Rômulo Ribeiro Pieroni

Div. de Metalurgia Nuclear: Prof. Tharcisio D.S. Santos

Div. de Engenharia Química: Prof. Kazimierz J. Bril

PARAMAGNETIC STUDIES OF HOLMIUM BY NEUTRON TOTAL CROSS SECTION MEASUREMENTS

Marieta C. Mattos

Nuclear Physics Division, Instituto de Energia Atômica,
Cidade Universitária, São Paulo, Brasil

RESUMO

Foi medida a secção de choque total do hólmio, para neutrons de comprimentos de onda entre 0,20 e 9,00 Angstroms . Foi usado o espectrômetro de cristal do IEA acoplado a um seletor mecânico de velocidade para eliminar reflexões de ordem superior do cristal. Amostras de Ho_2O_3 em pó foram preparadas em alto grau de pureza, tomando-se cuidado especial em eliminar contaminação por terras raras de alta secção de choque, para neutrons. Ainda que os fatores de forma paramagnética sejam usualmente determinados por medidas de secção de choque diferencial para neutrons de um único comprimento de onda, medidas precisas da secção de choque total num grande intervalo de comprimentos de onda conhecidos dão informações definidas sôbre o raio da órbita eletrônica 4f. Nossas medidas indicam um raio diferente daquele usado por Blume, Freeman e Watson, que calcularam o fator de forma assumindo funções de onda hidrogênicas. Será discutida a possível escolha de diferentes constantes de screening.

RESUME

La section efficace totale de l'holmium a été mesurée pour les neutrons de longueur d'onde entre 0,20 et 9,00 Angstroms. Le spectromètre à cristal de l'IEA a été employé acouplé à un

sélecteur mécanique de vitesse pour éliminer les réflexions d'ordre supérieur du cristal. Des échantillons de Ho_2O_3 en poudre ont été preparés avec haute pureté, en faisant spécialement attention pour éliminer la contamination par des terres rares de haute section efficace pour les neutrons. Bien que les facteurs de forme soient ordinairement déterminés par des mesures de section efficace différentielle à une seule longueur d'onde du neutron, des mesures précises de la section efficace totale dans un large intervalle de longueurs d'onde connues donnent des informations définies sur le rayon de l'orbite electronique 4f. Nos mesures indiquent un rayon différent de celui employé par Blume, Freeman et Watson, qui ont calculé le facteur de forme en assumant des fonctions d'onde hydrogéniques. Il sera discuté le choix possible de différentes constantes de screening.

ABSTRACT

The total neutron cross section for holmium was measured for neutron wavelengths between 0.20 and 9.00 Angstroms. The IEA crystal spectrometer was used together with a mechanical velocity selector to eliminate higher order reflections from the crystal. Powder samples of Ho_2O_3 were prepared in high purity, taking particular care to eliminate contamination by the rare earths of high neutron cross section. Although paramagnetic form factors are usually determined by differential cross section measurements with one neutron wavelength, accurate total cross section measurements for a wide range of known wavelengths give definite information on the radius of the 4f electron orbits. Our measurements indicate a radius different from the one used by Blume, Freeman and Watson, who calculated the form factor assuming hydrogenic wave functions. The possible choise of different screening constant will be discussed.

I. INTRODUCTION

During a program of total cross section measurements of the rare earth elements at this Institute, holmium was given special attention because of the interesting interaction between the neutrons and the atomic electrons. This paramagnetic scattering has been noticed before in total neutron cross sections by Bernstein et al.[1] and in neutron diffraction work by Koehler, Wollan and Wilkinson[2].

The total neutron cross section for scattering of neutrons by an atom in the presence only of an interaction between the magnetic moment of the neutron, γ, and that of the atom, μ, is

$$\sigma_{pm} = \frac{2}{3}\pi \left(\frac{e^2}{mc^2}\right)^2 \gamma^2 \mu^2 \overline{f^2} \quad ,$$

where $\frac{e^2}{mc^2}$ is the classical electron radius, and f is the neutron scattering form factor for those unpaired electrons which contribute to the magnetic moment of the holmium ion.

The magnetic moment of the holmium ion has been measured as being 10.34 ± .10 Bohr magnetons by Strandburg, Legvold and Spedding[3]. The paramagnetic scattering form factor has been calculated by Blume, Freeman and Watson[4], using Hartree - Fock wave functions for isolated ions. These form factors, together with known values of the neutron and ionic magnetic moments, may be used to predict the paramagnetic scattering component to the neutron scattering.

However, it is essential to make accurate measurements of the neutron cross section to supply information unavailable from the theory. In particular, the ionic form factor for the ion in the solid state may be expected to be different from the one for

a free ion. In addition, measurements over a wide range of neutron energies are required to determine the variations of the nuclear cross sections with neutron energy.

Ordinarily, scattering form factors are best determined by differential scattering experiments. Holmium has been measured in this way by Koehler, Wollan and Wilkinson[2]. In the present work, it is shown that careful total cross section measurements, besides giving the nuclear cross sections, give information about the 4f electron orbits.

II. EXPERIMENTAL METHOD

The source of neutrons for this work was the Instituto de Energia Atômica swimming pool research reactor operated at 2 Mw. The thermal neutron flux measured with gold foils near the core of the reactor is 2.4×10^{12} neutrons/cm^2/sec.

A crystal spectrometer and a mechanical velocity selector, constructed in the shops of the Instituto de Energia Atômica , were used as monochromators. Order contamination was eliminated from the beam by using the crystal together with the mechanical velocity selector.

The crystal spectrometer was first located close to the reactor in a radial beam-hole, as shown in Figure 1. Later, the crystal and the selector were located at one of the tangential beam-holes, as shown in Figure 2. We had a thermal flux of 4×10^6 neutrons/cm^2/sec. outside the radial port and of 1.4×10^8 neutrons/cm^2/sec. outside the tangential port. The crystal spectrometer angles were read on a vernier scale with a precision of 0.01 degree. The measurements were made with crystals of calcite, aluminium and mica. With the calcite

crystal the resolution was 18 minutes.

The mechanical velocity selector[5] gives a neutron energy with a resolution which depends on the rotation velocity, and on the helical channel inclination. We used a resolution of 50% in wavelength. The final resolution was determined by the crystal spectrometer and order contamination was completely eliminated by the mechanical velocity selector.

Commercial boron tri-fluoride detectors, enriched in the isotope B^{10}, were used for neutron detection.

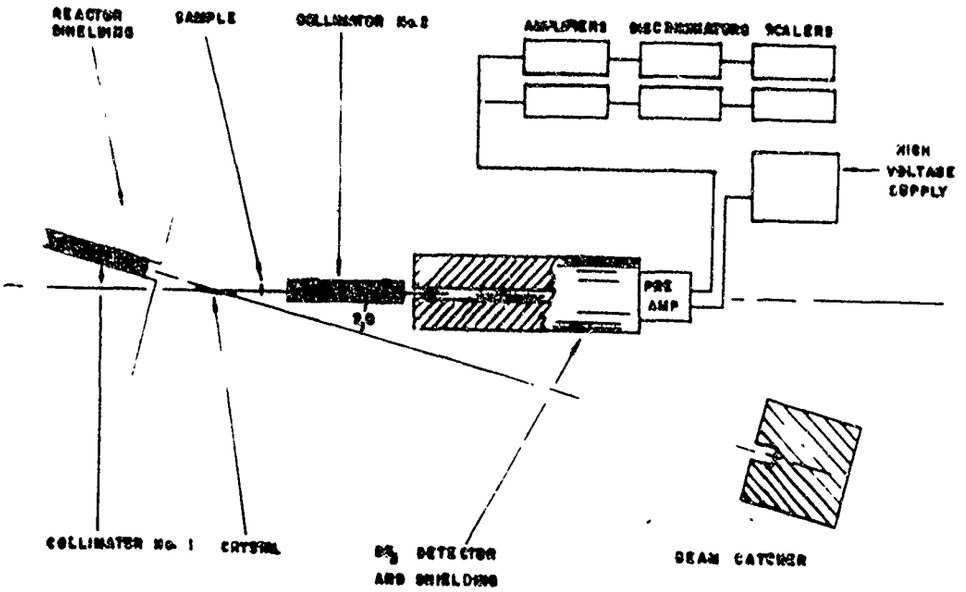

Figure 1 - Schematic diagram of the crystal spectrometer

The samples of holmium oxide were supplied by the Chemical Engineering Division of this Institute. The separation method employed, using ion exchange resins, assured us of the degree

of purification necessary for this experiment.

The samples were placed in aluminium containers and introduced into the beam in a reproducible position. The transmission through the sample was obtained by measuring the counting rate with the sample in the beam, and the rate obtained with an identical empty sample holder in the beam. A background was subtracted from each counting. The containers were designed to give a transmission which minimized the time required to reduce the statistical errors[6].

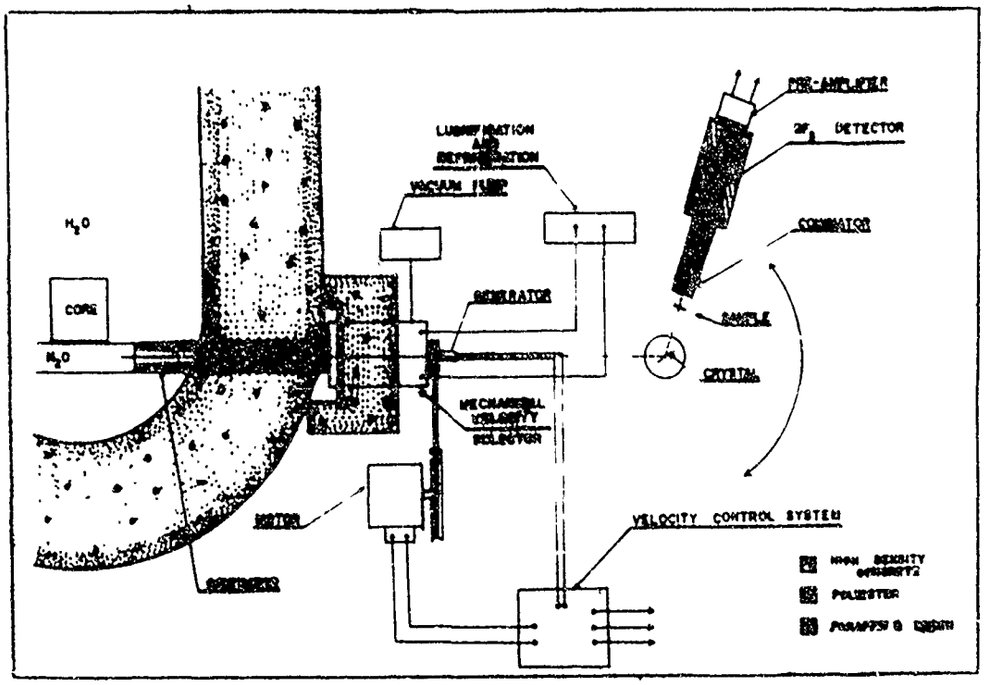

Figure 2 - Schematic diagram of the mechanical velocity selector together with the crystal spectrometer.

To avoid the influence on the transmission of the fluctuations of the reactor power and the instability of the

electronic circuits, the transmission measurements were repeated several times in cycles, according to a routine designed to cancel linear drifts. The detector pulses were amplified, analyzed and counted by two independent electronic systems.

The total cross sections were calculated from the transmission measurements. The conventional formula has been used for the error. The calculations were made by an IBM-1620 computer. The correction due to oxygen was made simply by subtracting the free atom oxygen cross section of 3,8 barns per atom. Figure 3 shows the results in the usual way with total cross section versus neutron energy.

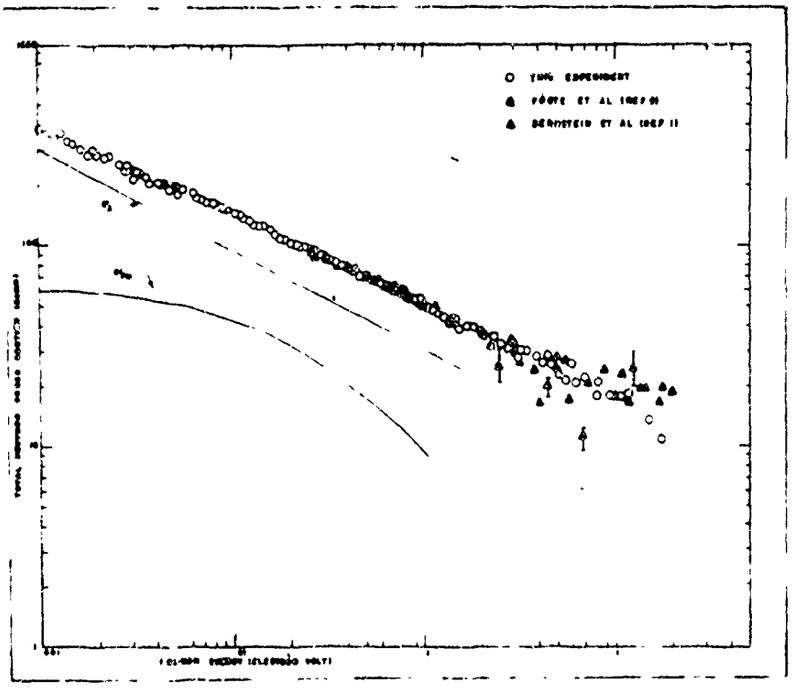

Figure 3 - Total neutron cross section of holmium as a function of neutron energy. The absorption cross section, σ_a, which is dependant on $1/\sqrt{E}$, and the calculated paramagnetic cross section, σ_{pm}, are shown.

Figure 4, with total cross section versus neutron wavelength, shows the same data, together with the paramagnetic scattering calculated from the form factors of Blume, Freeman and Watson[4].

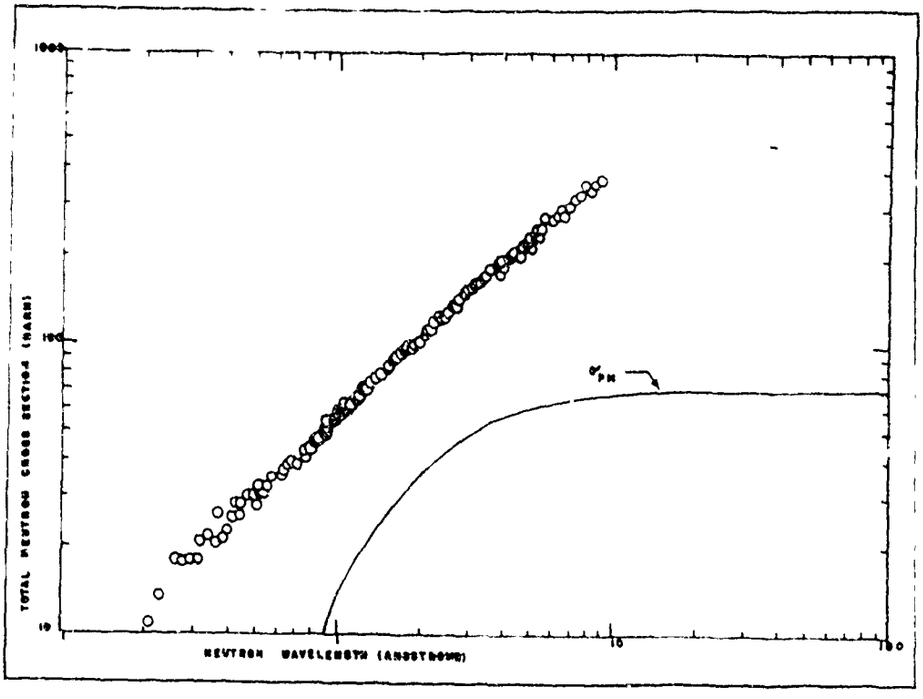

Figure 4 - Total neutron cross section of holmium as a function of neutron wavelength. The calculated paramagnetic cross section, σ_{pm}, is shown.

III. ANALYSIS OF DATA

The total cross section of holmium, σ_T, consists of three completely independent partial cross sections, one of which is the paramagnetic scattering, σ_{pm}. Then,

$$\sigma_T = \sigma_s + \sigma_a + \sigma_{pm} \quad ,$$

where σ_s and σ_a are the nuclear scattering and absorption, respectively. σ_s was assumed to be independent of energy and σ_a was assumed to vary as $1/\sqrt{E}$ over the range of this experiment. The nuclear resonance spacing is about 6 electron volts[7]. The first resonance at 3.92 electron volts has no effect on these assumptions. It is unlikely that a bound state would influence the dependence on energy of the nuclear cross sections.

Nuclear scattering contributes least to our experimental data. For the purpose of analysis, σ_s was taken as 7 barns by comparing with neighbouring nuclei[7]. Nuclear absorption dominates at very low energies and may be quite well determined by using the asymptotic value of $\sigma_{pm} = 65.2 \pm 1.3$ barns, calculated from the holmium ion magnetic moment.

The nuclear absorption cross section thus determined from our data is $\sigma_a = 61 \pm 3$ barns, reduced to its value at thermal neutron energy .025 electron volts.

IV. CONCLUSIONS

Figure 5 shows our experimental points after having subtracted the contributions of nuclear scattering and absorption.

Comparing our experimentally determined paramagnetic scattering cross section with that expected from the Hartree--Fock calculations of Blume, Freeman and Watson[4] one sees that the disagreement is not serious. A 4f shell radius smaller by 10%, or a screening constant 5% less, would minimize the discrepancy between their theory and our results. However, an agreement within experimental errors cannot be obtained only by changing the radius, but rather by admitting the possibility of

a slightly more diffuse wave function, such as proposed by Judd and Lindgren[8]. Unfortunately, no paramagnetic neutron scattering form factors are available using their wave functions.

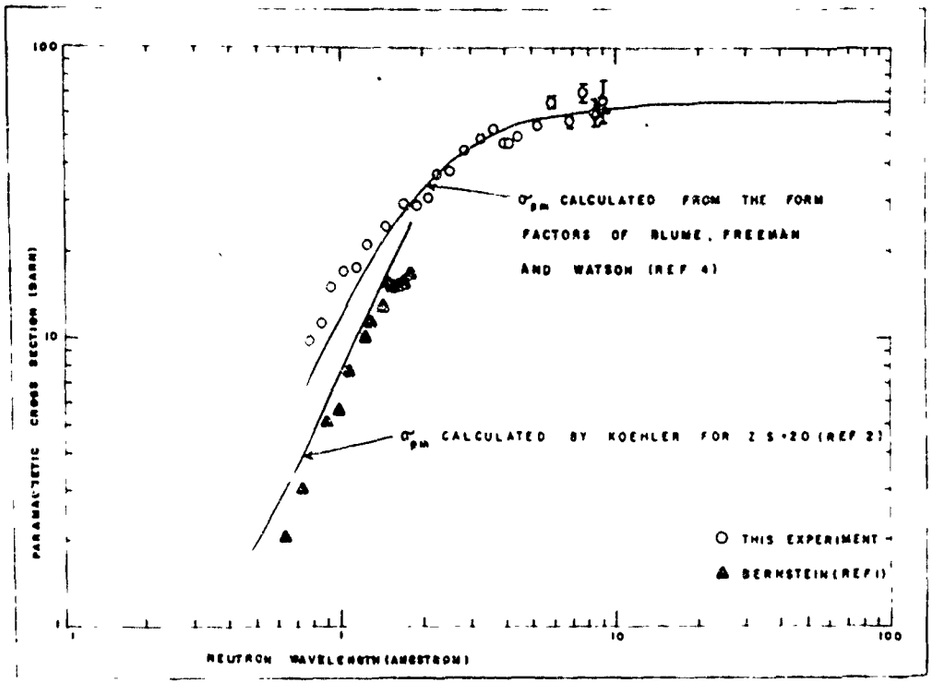

Figure 5 - Comparison between the experimental paramagnetic cross section, obtained after having subtracted the contribution of nuclear scattering and absorption, and the theoretical paramagnetic cross section, calculated from the form factors of Blume, Freeman and Watson[4]. The older theory quoted by Koehler et al[2] is shown. The apparently discrepant points due to Bernstein et al[1] are explained in the text.

The determined values of σ_{pm} of Bernstein et al.[1] are different from ours although Figure 3 shows that the total cross sections agree in the region where their statistical errors were comparable with ours. Their paramagnetic cross sections differs

from our values which have taken advantage of more recent available information. Their results were corrected using a nuclear scattering cross section of 13 barns, based on a total cross section of 28 barns at 0.5 eV. It now appears from the compilation of all total cross section values that 28 barns is at least 3 barns too high, as it can be seen in Figure 3. In addition, they neglected the effects of the then unknown 3.92 eV resonance on the capture cross section at 0.5 eV (about 1 barn), and they underestimated (by about 1 barn) the paramagnetic scattering cross section at 0.5 eV. Taken together, their estimate of 13 barns for nuclear scattering is about 5 barns too high. In our lower energy range, the nuclear scattering is relatively unimportant; in the absence of direct measurements, we used 7 barns based on measured values of nuclear radii of neighbouring nuclei[10]. Finally, analysis with our new value of the thermal absorption cross section of 61 ± 3 barns instead of 64 assumed by Bernstein et al. accounts for the remaining small discrepancy between the analysis of our results and that of their careful measurements.

Figure 5 also shows the disagreement between the older calculation quoted in the experimental work of Koehler et al.[2], who used the theory by Trammell[11] with hydrogen-like wave functions, and the calculation of Blume, Freeman and Watson[4] who used the same theory with Hartree-Fock wave functions. Blume, Freeman and Watson noted this disagreement. The interpretation of our results, according to Trammell's theory, favours the smaller 4f shell implied by the more recent calculations of Blume, Freeman and Watson.

We plan to continue our work with metallic samples to eliminate small uncertainties in subtracting the scattering by oxigen. In addition, it is planned to make an independent measurement of the nuclear absorption cross section with

facilities existing in this Institute.

V. ACKNOWLEDGMENTS

The author wishes to express her sincere thanks to Dr. R.L. Zimmerman for helpful suggestions. She is also greatly indebted to Dr. N. Nereson for his interest and encouragement, to Dr. K.J. Bril for supplying samples of high purity, and to S. Herdade, R. Fulfaro and R. Stasiulevicius who have made most of the measurements.

VI. BIBLIOGRAPHY

1. Bernstein, S., Borst, L.B. Stanford, C.P., Stephenson, T.E. and Dial, J.B., Phys. Rev. 87, 487 (1952).
2. Koehler, W.C., Wollan, E.O. and Wilkinson, M.K., Phys. Rev. 110, 37 (1958).
3. Strandburg, D.L., Legvold, S., and Spedding, F.H.. Phys.Rev. 127, 2046 (1958).
4. Blume, M., Freeman, A.J., and Watson, R.E., J. Chem. Phys. 37, 1245 (1962).
5. Bianchini, F.G., Abreu, M., Amaral, L.Q., and Martins, O.W. , Instituto de Energia Atômica Publication Nº 78 (November 1964).
6. Rose, M.E., and Shapiro, M.M., Phys. Rev. 74, 1853 (1948).
7. Hughes, D.J., and Schwartz, R., Neutron Cross Section (U.S. Government Printing Office, Washington, D.C., 1958).
8. Judd, B.R., and Lindgren, I., Phys. Rev. 122, 1802 (1961).
9. Focte, H.L.,Landon, H.H., and Sailor, V.L., Phys. Rev. 92, 656 (1953).
10. Seth, K.K., Hughes, D.L., Zimmerman, R.L., and Garth, R., Phys. Rev. 110, 692 (1958).
11. Trammell, G.T., Phys. Rev. 92, 1387 (1953).

UNCLASSIFIED
Security Classification

DOCUMENT CONTROL DATA – R&D

(Security classification of title, body of abstract and indexing annotation must be entered when the overall report is classified)

1 ORIGINATING ACTIVITY *(Corporate author)*
Iowa State University
Department of Physics
Ames, Iowa

2A REPORT SECURITY CLASSIFICATION
☒ Unclassified
☐ Other — Specify

2B. GROUP

3 REPORT TITLE
Rare Earth Research Conference 5th Ames, Iowa 30 Aug-1 Sep 1965 Books 1-6. Spectra Bk 1; Solid State Bks 2,4 & 6; Chemistry Bk 3; Metallurgy Bk 5

4 DESCRIPTIVE NOTES *(Type of report and inclusive dates)*
☐ Scientific Report ☒ Final Report ☐ Journal Article ☐ Proceedings ☐ Book

5 AUTHOR(S) *(Last name, first name, initial)*
- - -
(Legvold Sam Dr (PI)

6. REPORT DATE AS PRINTED	7A. TOTAL NO. OF PAGES	7B. NO. OF REFS
September 1965	718	311

8A CONTRACT OR GRANT NO. AF-AFOSR-812-65
B. PROJECT NO. 9760-01
C. 61445014
D.

9A. ORIGINATOR'S REPORT NUMBER(S) *(If given)*

9B. OTHER REPORT NO.(S) *(Any other numbers that may be assigned this report)*
AFOSR 65-1917
AD

10 AVIALABILITY/LIMITATION NOTICES
Distribution of this document is unlimited

☒ Available from DDC
☒ Available from CFSTI
☐ Available from Source
☐ Available Commercially

11. SUPPLEMENTARY NOTES *(Citation)*

12. SPONSORING MILITARY ACTIVITY
AF Office of Scientific Research (SRC)
Office of Aerospace Research
Washington, D. C. 20333

13 ABSTRACT

A total of 69 papers were presented at the Rare Earth Research Conference. The papers, with abstracts, are contained in 6 volumes. Book 1 deals with spectra; Books 2, 4, and 6, solid state; Book 3, chemistry; and Book 5, metallurgy. (U)

DD FORM 1473
1 JAN 64

UNCLASSIFIED
Security Classification

Security Classification

14 KEY WORDS	LINK A		LINK B		LINK C		LINK D	
	ROLE	WT	ROLE	WT	ROLE	WT	ROLE	WT
Metallurgy Rare Earth Elements Solid States Spectra Symposia								

INSTRUCTIONS

1. ORIGINATING ACTIVITY. Enter the name and address of the contractor, subcontractor, grantee, Department of Defense activity or other organization *(corporate author)* issuing the report.

2a. REPORT SECURITY CLASSIFICATION: Enter the overall security classification of the report. Indicate whether "Restricted Data" is included. Marking is to be in accordance with appropriate security regulations.

2b. GROUP: Automatic downgrading is specified in DoD Directive 5200.10 and Armed Forces Industrial Manual. Enter the group number. Also, when applicable, show that optional markings have been used for Group 3 and Group 4 as authorized.

3. REPORT TITLE: Enter the complete report title in all capital letters. Titles in all cases should be unclassified. If a meaningful title cannot be selected without classification, show title classification in all capitals in parenthesis immediately following the title.

4. DESCRIPTIVE NOTES: If appropriate, enter the type of report, e.g., interim, progress, summary, annual, or final. Give the inclusive dates when a specific reporting period is covered.

5. AUTHOR(S): Enter the name(s) of author(s) as shown on or in the report. Enter last name, first name, middle initial. If military, show rank and branch of service. The name of the principal author is an absolute minimum requirement.

6. REPORT DATE: Enter the date of the report as day, month, year; or month, year. If more than one date appears on the report, use date of publication.

7a. TOTAL NUMBER OF PAGES: The total page count should follow normal pagination procedures, i.e., enter the number of pages containing information.

7b. NUMBER OF REFERENCES: Enter the total number of references cited in the report.

8a. CONTRACT OR GRANT NUMBER: If appropriate, enter the applicable number of the contract or grant under which the report was written.

8b, 8c, & 8d. PROJECT NUMBER: Enter the appropriate military department identification, such as project number, subproject number, system numbers, task number, etc.

9a. ORIGINATOR'S REPORT NUMBER(S): Enter the official report number by which the document will be identified and controlled by the originating activity. This number must be unique to this report.

9b. OTHER REPORT NUMBER(S): If the report has been assigned any other report numbers (either by the originator or by the sponsor), also enter this number(s).

10. AVAILABILITY/LIMITATION NOTICES: Enter any limitations on further dissemination of the report, other than those imposed by security classification, using standard statements such as:

(1) "Qualified requesters may obtain copies of this report from DDC."

(2) "Foreign announcement and dissemination of this report by DDC is not authorized."

(3) "U. S. Government agencies may obtain copies of this report directly from DDC. Other qualified DDC users shall request through

_____."

(4) "U. S. military agencies may obtain copies of this report directly from DDC. Other qualified users shall request through

_____."

(5) "All distribution of this report is controlled. Qualified DDC users shall request through

_____."

If the report has been furnished to the Office of Technical Services, Department of Commerce, for sale to the public, indicate this fact and enter the price, if known.

11. SUPPLEMENTARY NOTES: Use for additional explanatory notes.

12. SPONSORING MILITARY ACTIVITY: Enter the name of the departmental project office or laboratory sponsoring *(paying for)* the research and development. Include address.

13. ABSTRACT: Enter an abstract giving a brief and factual summary of the document indicative of the report, even though it may also appear elsewhere in the body of the technical report. If additional space is required, a continuation sheet shall be attached.

It is highly desirable that the abstract of classified reports be unclassified. Each paragraph of the abstract shall end with an indication of the military security classification of the information in the paragraph, represented as *(TS), (S), (C), or (U)*

There is no limitation on the length of the abstract. However, the suggested length is from 150 to 225 words.

14. KEY WORDS: Key words are technically meaningful terms or short phrases that characterize a report and may be used as index entries for cataloging the report. Key words must be selected so that no security classification is required. Identifiers, such as equipment model designation, trade name, military project code name, geographic location, may be used as key